Evolutionary reconstruction of the retromer complex and its function in *Trypanosoma brucei*

V. Lila Koumandou[1], Mary J. Klute[2], Emily K. Herman[2], Ricardo Nunez-Miguel[3], Joel B. Dacks[2,*] and Mark C. Field[1,*]

[1]Department of Pathology, University of Cambridge, Tennis Court Road, Cambridge CB2 1QT, UK
[2]Department of Cell Biology, University of Alberta, Edmonton, AB T6G 2H7, Canada
[3]Department of Biochemistry, University of Cambridge, Tennis Court Road, Cambridge CB2 1QT, UK
*Authors for correspondence (dacks@ualberta.ca; mcf34@cam.ac.uk)

Accepted 22 December 2010
Journal of Cell Science 124, 1496-1509

doi:10.1242/jcs.081596

Summary

Intracellular trafficking and protein sorting are mediated by various protein complexes, with the retromer complex being primarily involved in retrograde traffic from the endosome or lysosome to the Golgi complex. Here, comparative genomics, cell biology and phylogenetics were used to probe the early evolution of retromer and its function. Retromer subunits Vps26, Vps29 and Vps35 are near universal, and, by inference, the complex was an ancient feature of eukaryotic cells. Surprisingly, we found DSCR3, a Vps26 paralogue in humans associated with Down's syndrome, in at least four eukaryotic supergroups, implying a more ancient origin than previously suspected. By contrast, retromer cargo proteins showed considerable interlineage variability, with lineage-specific and broadly conserved examples found. Vps10 trafficking probably represents an ancestral role for the complex. Vps5, the BAR-domain-containing membrane-deformation subunit, was found in diverse eukaryotes, including in the divergent eukaryote *Trypanosoma brucei*, where it is the first example of a BAR-domain protein. To determine functional conservation, an initial characterisation of retromer was performed in *T. brucei*; the endosomal localisation and its role in endosomal targeting are conserved. Therefore retromer is identified as a further feature of the sophisticated intracellular trafficking machinery of the last eukaryotic common ancestor, with BAR domains representing a possible third independent mechanism of membrane-deformation arising in early eukaryotes.

Key words: DSCR3, Evolution, Golgi complex, Intracellular trafficking, Phylogeny, Protocoatomer

Introduction

Intracellular trafficking and protein sorting mechanisms direct delivery of cargo throughout eukaryotic cells (Bonifacino and Glick, 2004). Cargo selection for transport and packaging into carrier intermediates is performed by several coat complexes. The 'endosomal sorting complex required for transport' (ESCRT) is responsible for inward budding of vesicles at the multi-vesicular body (Hurley, 2008), whereas COPI, COPII and clathrin–adaptin complexes mediate outward membrane budding (Bonifacino and Glick, 2004). These latter three coat complexes share a similar mechanism of action, requiring a GTPase and activator, plus effector proteins selecting cargo. Further subunits within each complex share a β-propeller–α-solenoid secondary structure, and there is evidence for distant evolutionary relationships (Devos et al., 2004). Together with the targeting and fusion machinery of Rabs, SNAREs and tethering proteins, vesicle coats are key determinants of trafficking specificity (Cai et al., 2007).

Retromer, a further coat complex is present in animal and fungal cells, but it bears no obvious relationship to ESCRT or protocoatomer. Its best-characterised function is recycling of vacuolar hydrolase receptors (Seaman et al., 1998; Nothwehr et al., 2000) in yeast and cation-independent mannose 6-phosphate receptors in mammals (Arighi et al., 2004). Retromer is also implicated in the trafficking of additional proteins, including the polymeric immunoglobulin receptor (Verges et al., 2004), plasma membrane iron transporters (Strochlic et al., 2007), wntless (Eaton, 2008) and the Shiga and Cholera toxins (Bujny et al., 2007; Popoff et al., 2007), and in the processing of the amyloid precursor protein (He et al., 2005). Additionally, retromer is implicated in clearing apoptotic bodies (Chen et al., 2010) and trafficking from the mitochondria to peroxisomes (Braschi et al., 2010), underlying diverse roles.

Saccharomyces cerevisiae retromer is composed of at least five proteins: Vps5, Vps17, Vps26, Vps29 and Vps35 (Seaman et al., 1998). Mutants exhibit variable deficiencies, with highly fragmented vacuoles in Vps5 and Vps17 mutants, moderate fragmentation in Vps26 mutants (Raymond et al., 1992) and no morphological defects for Vps29 and Vps35 mutants. In mammals, retromer composition is similar and the complex contains orthologues of Vps26, Vps29 and Vps35 (Haft et al., 2000). Vps29 is homologous to prokaryotic pyrophosphatases but probably lacks nucleosidase activity (Collins, 2008; Collins et al., 2005; Damen et al., 2006). Vps35 and Vps26 bind cargo at endosomal membranes (Nothwehr et al., 1999; Reddy and Seaman, 2001). The mammalian counterparts of Vps5 and Vps17 are the sorting nexin (SNX) proteins SNX1, SNX2, SNX5 and SNX6 (Carlton et al., 2005; Wassmer et al., 2007). Although direct orthology with Vps5 and Vps17 has not been demonstrated, the sorting nexins possess the lipid-binding phox (PX) and BAR domains, which might enable a function in membrane deformation following cargo recruitment (Wassmer et al., 2009). SNX1 and SNX2 self-assemble and colocalise with the endosomal markers EEA1 and Rab5 (Haft et al., 1998; Kurten et al., 1996; Kurten et al., 2001; Teasdale et al., 2001). In mouse, *SNX1* and *SNX2* double-knockouts cause arrest of embryonic development (Schwarz et al., 2002), and transcriptome analysis implicates Vps35 in Alzheimer's disease,

underlining the importance of retromer to mammalian systems (Griffin et al., 2005; Small et al., 2005).

Membrane trafficking appears to be an ancient and important innovation for the earliest eukaryotes (Dacks and Field, 2007). Comparative genomics and phylogenetics (Dacks and Field, 2007; Field and Dacks, 2009) reveal unexpected complexity in trafficking machinery in the Last Eukaryotic Common Ancestor (LECA). COPI, COPII and clathrin–adaptin coats are conserved across eukaryotes (Dacks and Field, 2004); their similar mechanisms of action are reflected in shared structures as they possess a β-propeller, α-solenoid organisation and are predicted to have arisen from a primordial protocoatomer complex (deGrasse et al., 2009). The ESCRT complex is clearly independent from protocoatomer (Field and Dacks, 2009), yet the core components of ESCRT are conserved across eukaryotes (Leung et al., 2008), implying that the ancestor possessed at least two independent membrane-deformation mechanisms.

Retromer homologues are present in many eukaryotes, suggesting an ancient origin, with tentative evidence for a relationship with protocoatomer coats (Dacks et al., 2009). However, no systematic analysis of retromer across eukaryotic diversity and no investigation of the evolutionary history of retromer subunits had been undertaken.

We used comparative genomics, across organisms representing all eukaryotic supergroups, to obtain sequences encoding retromer components and all reported cargo proteins. This was combined with functional characterisation in *Trypanosoma brucei* to validate in silico predictions and explore conservation of function in an organism highly divergent from animals and yeast.

Results

Retromer is a universal eukaryotic feature

In yeast, retromer comprises Vps26, Vps29 and Vps35, forming a cargo-selective subcomplex, and Vps5 and Vps17, which act as the membrane deforming coat. We found that the cargo-selection subcomplex was extremely well conserved, probably reflecting near universal importance (Fig. 1). The only candidate for secondary loss was *Ostreococcus tauri*, where we failed to identify Vps29. However, given the extremely high conservation this absence might be due to high sequence divergence in *O. tauri* or absence from the available genome assembly. Interestingly, all cargo-selection subunits showed expansions in some lineages; Vps26 was the most widely expanded, with multiple homologues in at least one organism from each supergroup (Fig. 1). Phylogenetic analysis indicated that most expansions were species-specific,

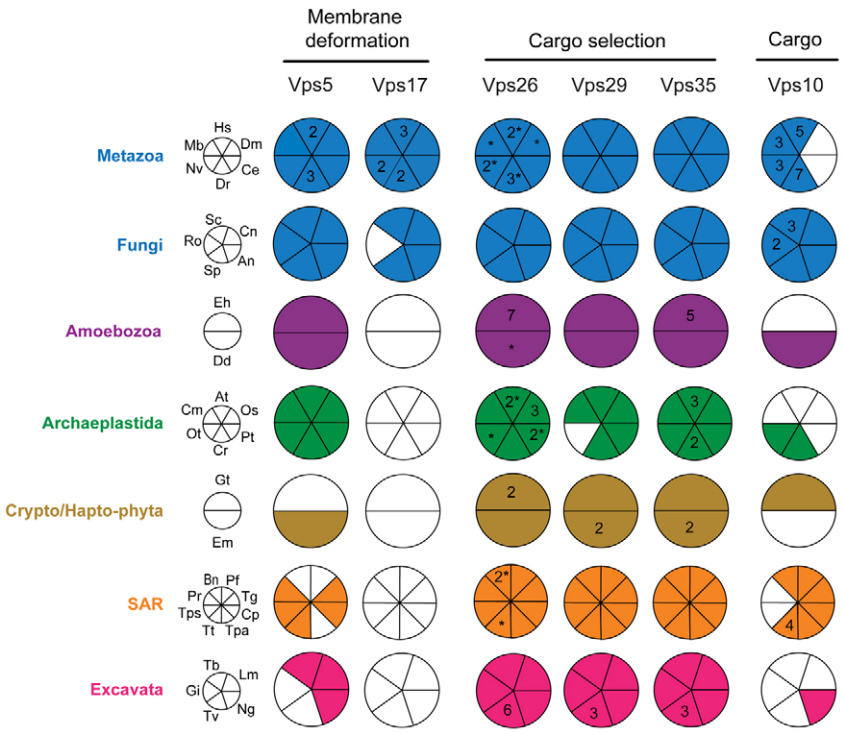

Fig. 1. Distribution of retromer components across eukaryotic lineages. Most retromer components are conserved across eukaryotes, except Vps17, which is restricted to opisthokonts. Vps5 and Vps10 are frequently lost. The factors are named using *S. cerevisiae* nomenclature. Large taxon groupings are colour coded, and a diagram defining the species represented is given. Data are based on BLAST and HMMer results together with alignments and phylogenetics. Filled sectors indicate the presence of the protein (see Materials and Methods) and white sectors indicate that the protein was not found. The numbers in the sectors indicate that multiple copies of factors were found (the products of distinct genes). The asterisks in the Vps26 column indicate the presence of a DSCR3 homologue and a Vps26-encoding gene. The accession numbers are given in supplementary material Table S1. Species abbreviations: Opisthokonts (blue): Hs, *Homo sapiens*; Dm, *Drosophila melanogaster*; Ce, *Caenorhabditis elegans*; Dr, *Danio rerio*; Nv, *Nematostella vectensis*; Mb, *Monosiga brevicollis*; Sc, *Saccharomyces cerevisiae*; Cn, *Cryptococcus neoformans*; An, *Aspergillus nidulans*; Sp, *Schizosaccharomyces pombe*; Ro, *Rhizopus oryzae*. Amoebozoa (purple): Eh, *Entamoeba histolytica*; Dd, *Dictyostelium discoideum*. Archaeplastida (green): At, *Arabidopsis thaliana*; Os, *Oryza sativa*; Pt, *Populus trichocarpa*; Cr, *Chlamydomonas reinhardtii*; Ot, *Ostreococcus tauri*; Cm, *Cyanidioschyzon merolae*. Crypto- and Hapto-phyta (bronze): Gt, *Guillardia theta*; Em, *Emiliania huxleyi*. Stramenopile-Alveolate-Rhizaria (i.e. SAR) (orange): Pf, *Plasmodium falciparum*; Tg, *Toxoplasma gondii*; Cp, *Cryptosporidium parvum*; Tpa, *Theileria parva*; Tt, *Tetrahymena thermophila*; Tps, *Thalassiosira pseudonana*; Pr, *Phytophthora ramorum*; Bn, *Bigelowiella natans*. Excavata (fuchsia): Tb, *Trypanosoma brucei*; Lm, *Leishmania major*; Ng, *Naegleria gruberi*; Tv, *Trichomonas vaginalis*; Gi, *Giardia intestinalis*. This convention is used throughout.

except for a possible duplication in the common ancestor of *Homo sapiens* and *Danio rerio* (Fig. 2).

Vps26 contains an arrestin N-terminal domain, and the Vps26-domain-containing family of proteins includes DSCR3 (Down syndrome critical region 3). DSCR3 is encoded by a gene associated with chromosome 21 trisomy characteristic of Down's syndrome and is associated with pathogenesis (Hu et al., 2006). In searches for Vps26, we identified homologues of DSCR3 in multiple lineages, suggesting an ancient origin, and phylogenetics identified a monophyletic clade for all DSCR3 homologues, originating before diversification of eukaryotic lineages (Fig. 2). However, retention of DCSR3 was limited, suggesting a requirement only in certain taxa, despite the ancestral origin. Such sparse retention has been noted for additional trafficking factors, for example, Rab4 (Field et al., 2007a).

Vps29 is part of the retromer cargo-recognition subcomplex and probably mediates binding of Vps26 to Vps35 and that between the cargo recognition and membrane targeting subcomplexes (Vps5 and Vps17 in yeast; SNX1 and SNX2 in mammals). There were multiple Vps29 homologues in *Emiliania huxleyi*, *Naegleria gruberi* and *Trichomonas vaginalis*, which were lineage-specific (Fig. 3). All identified Vps29 orthologues possessed a phosphatase domain (Collins, 2008; Collins et al., 2005), homologous with prokaryotic pyrophosphatases. Phylogenetic analysis of Vps29, and eubacterial and archaeal phosphatases sharing this domain, was used to further examine the prokaryotic origins of this subunit. Eukaryotic Vps29 formed a robust monophyletic clade distinct from prokaryotic pyrophosphatases (Fig. 3); the only exception, *Cyanidioschyzon merolae*, which grouped with prokaryotes, was probably due to high sequence divergence. Despite sampling a variety of archaeal and eubacterial homologues, a precise origin for Vps29 was not established, and the archaeal and eubacterial sequences did not form distinct clades, either due to horizontal gene transfer or the relatively short length of the Vps29 sequence resulting in insufficient resolution.

Multiple Vps35 homologues were found in *Nematostella vectensis*, *Entamoeba histolytica*, *Arabidopsis thaliana*, *Populus trichocarpa*, *E. huxleyi* and *T. vaginalis*. These expansions again appeared to be species-specific and thus relatively recent (Fig. 4).

Evolution of sorting nexins

The retromer membrane attachment subcomplex was also well conserved but significantly more variable than the cargo recognition complex (Fig. 1). Yeast and metazoan sorting nexins Vps5, Vps17, SNX1, SNX2, SNX3, SNX5 and SNX6 are suggested to be part of retromer (Griffin et al., 2005; Haft et al., 2000; Seaman et al., 1998; Strochlic et al., 2007; Wassmer et al., 2007). Because of this variability in components of the retromer, and as the evolution of sorting nexins has not been considered beyond opisthokonts (Cullen, 2008; Wassmer et al., 2009), we examined the broader

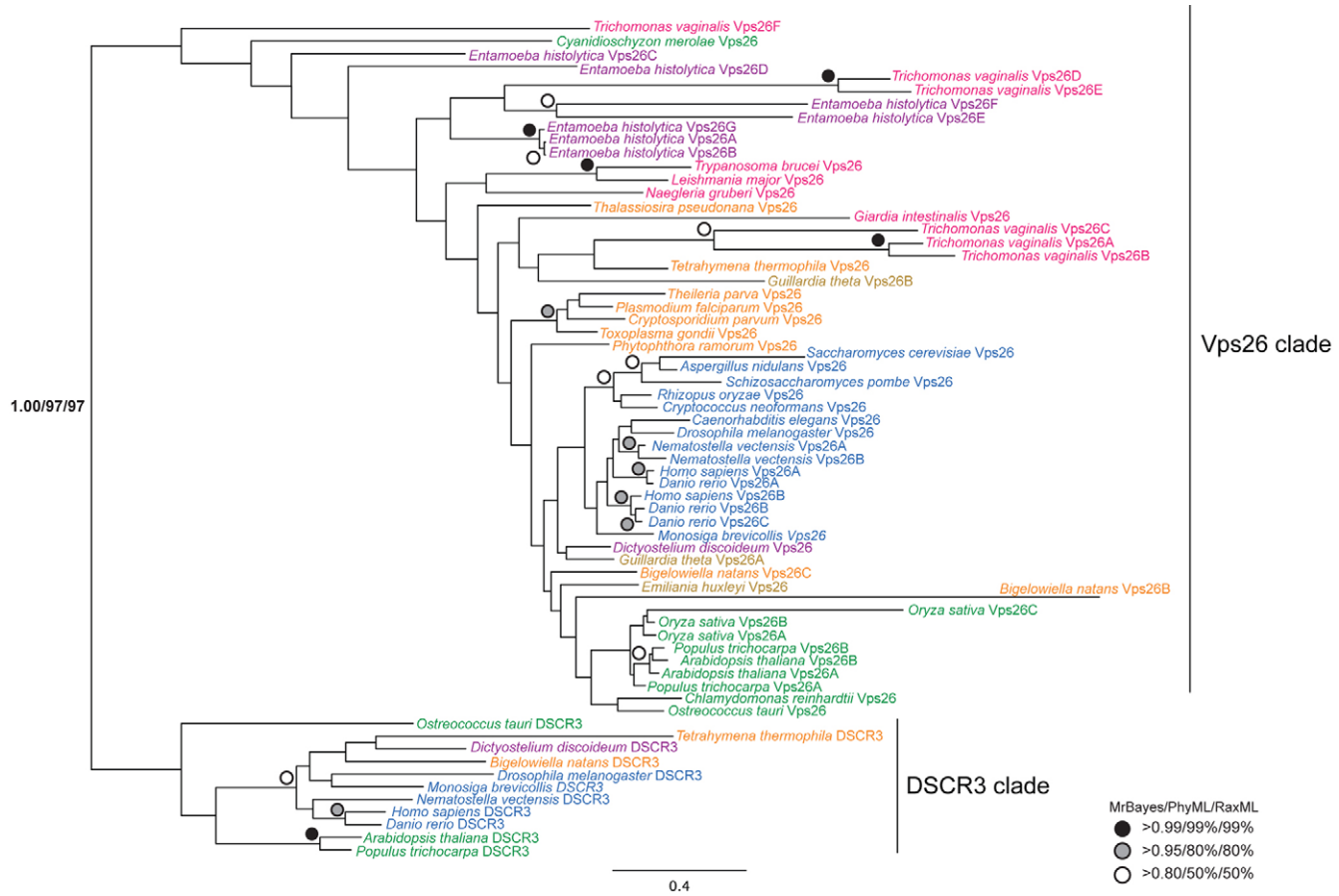

Fig. 2. Phylogenetic reconstruction of Vps26. The tree shown is the best Bayesian topology. Numerical values at the nodes of the tree (x/y/z) indicate statistical support by MrBayes, PhyML and RAxML (posterior probability, bootstrap and bootstrap, respectively). Values for highly supported nodes have been replaced by symbols as indicated. Species names are coloured as for the supergroups in Fig. 1. The DSCR3 clade is well-supported by all three methods, and indicates an early split between Vps26 and DSCR3 and many secondary losses.

evolution of sorting nexins (supplementary material Table S1, allSNX.R1). As reported previously, sorting nexins can be divided into three classes, with the overarching characteristic being the presence of a PX domain (Cullen, 2008). One class of sorting nexins contains only a PX domain and no additional defined domains (SNX-PX), another class contains proteins with a PX domain and a C-terminal BAR domain (SNX-BAR) and the third class of sorting nexins contain a PX domain and additional defined domain(s) excluding BAR (SNX-others). Kinases with PX domains were excluded, as they are not sorting nexins. Using an HMM profile of the 33 human sorting nexins, representing the three classes, we searched for sorting nexins across the eukaryotes. All three classes were well-conserved across eukaryotes (Fig. 5), although no sorting nexins were identified in *Guillardia theta*, *Plasmodium falciparum*, *Theileria parva*, *T. vaginalis* and *Giardia intestinalis* by our methods. Additional members of the supergroups to which these taxa belong did possess PX domain proteins, so this is probably secondary loss or sampling artefact. Bayesian and Maximum Likelihood phylogenetic analysis of all the SNX-PX and SNX-others sorting nexins failed to give robust resolution (data not shown). Therefore orthologues for Vps5 in Fig. 5 are restricted to the best relationship by BLAST analysis. However, phylogenetics of fungal sorting nexins established a close relationship for Vps5 and Vps17, to the exclusion of other sorting nexins (supplementary material Fig. S1).

Vps5, Vps17, SNX1, SNX2, SNX5 and SNX6 are all SNX-BAR sorting nexins and are proposed to function as heterodimers (Vps5–Vps17, SNX1–SNX2 and SNX5–SNX6) within retromer (Griffin et al., 2005; Haft et al., 2000; Seaman et al., 1998; Wassmer et al., 2007). The BAR domain functions in dimerisation and sensing membrane curvature, whereas the PX domain binds specific phosphoinositides and, hence, is important for targeting. Of the two sorting nexin subcomplex subunits in yeast, Vps5 was well conserved. As to the question of whether Metazoa possess a Vps17 orthologue, SNX2 was originally suggested (Carlton et al., 2005) and SNX5–SNX6 has been shown experimentally to be functionally equivalent (Wassmer et al., 2007); however, previous phylogenetic analysis failed to resolve the relationship between these proteins (Wassmer et al., 2009). We thus performed phylogenetic analysis of opisthokont SNX-BAR sorting nexins to resolve this issue. This indicated that metazoan SNX1 and SNX2 were both orthologous to yeast Vps5, refuting the hypothesis that SNX2 is orthologous to yeast Vps17 (Fig. 6). Furthermore, SNX1 and SNX2 probably resulted from a duplication of Vps5 in the vertebrate ancestor, whereas SNX5 and SNX6 resulted from a duplication of Vps17 in the metazoan ancestor (Fig. 6).

The sorting nexin of *Trypanosoma brucei* contains a BAR domain

Many species contained only one SNX-BAR sorting nexin (*Dictyostelium discoideum*, *Toxoplasma gondii*, *Trypanosoma*

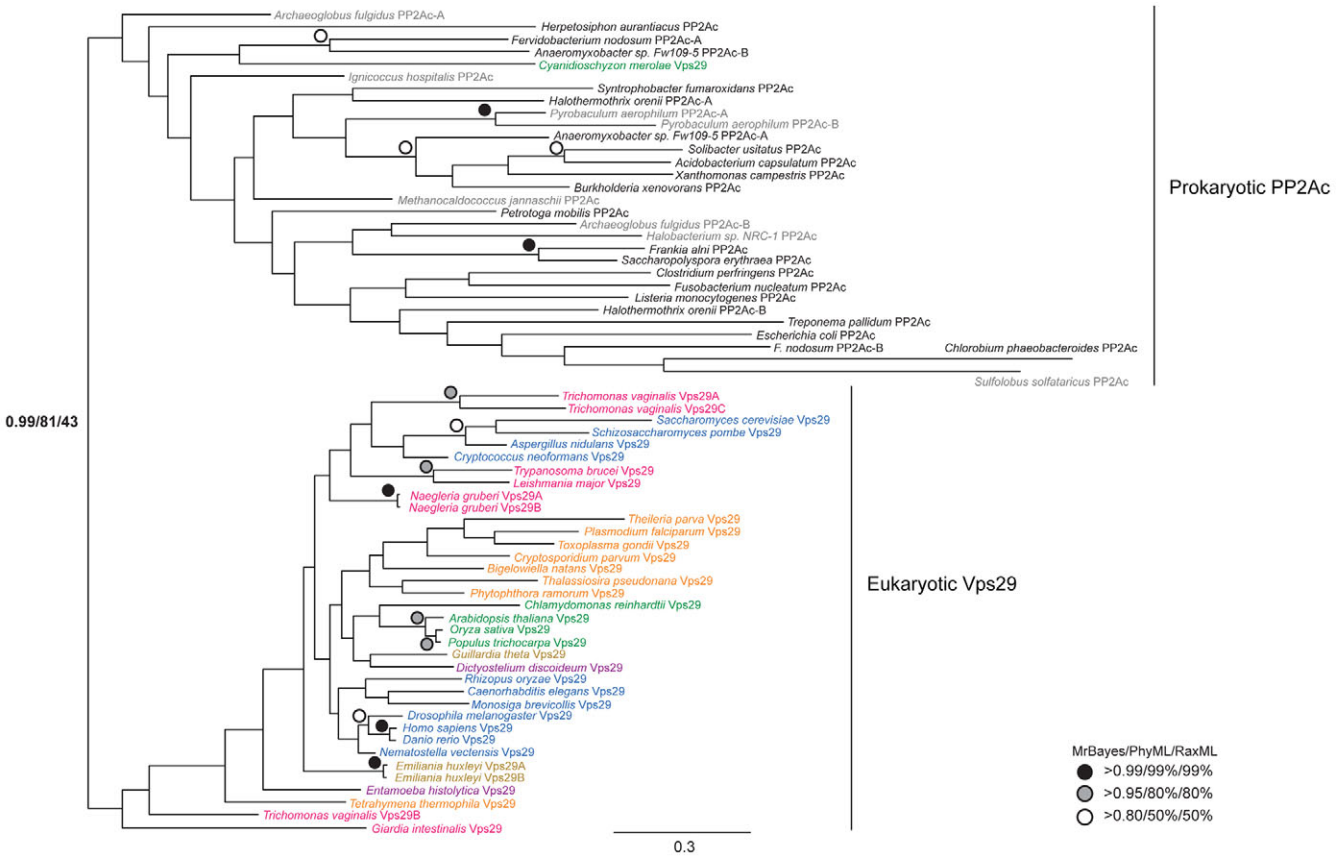

Fig. 3. Phylogenetic reconstruction of the Vps29 family in eukaryotes and prokaryotic pyrophosphatases. The tree shown is the best Bayesian topology. Supergroup colour codes are as for Fig. 1; the numerical values at the nodes of the tree and symbols for highly supported nodes are as in Fig. 2. Bacterial species names are shown in black, and archaea species names are shown in grey. The eukaryotes form a distinct and well-supported group, separate from the prokaryotes (apart from *C. merolae*, possibly due to high sequence divergence of the protein in this species), but the exact prokaryotic origin of Vps29 cannot be resolved, as the groupings within the prokaryotes are not well-supported.

brucei, *Leishmania major* and *N. gruberi*). As retromer in yeast and mammals possesses a sorting nexin dimer, potentially single SNX-BAR proteins could homodimerise. Furthermore, *T. brucei* was previously reported to lack the BAR domain (Berriman et al., 2005); as BAR domains might represent a distinct mechanism for membrane-deformation, we wished to establish whether the single trypanosome SNX-BAR indeed contained a BAR-related structure.

T. brucei Vps5 (Tb09.211.4240) contains a recognisable but divergent Vps5 Pfam domain belonging to the BAR domain family. To test whether this domain could function as a true BAR domain, aiding dimerisation and induction of membrane curvature, we constructed a model of the protein. The *T. brucei* Vps5 sequence was used to search for homologous protein structures in the Protein Data Bank. The phosphoinositide-binding PX and the BAR domains of human SNX9 (Pylypenko et al., 2007), identified as the appropriate homologue of *T. brucei* Vps5, were then used as the model template. The resulting model indicated that *T. brucei* Vps5 could indeed form a dimer through the Vps5 BAR domain and adopt a coiled-coil conformation similar to other sorting nexin dimers (Fig. 7). The model is predicted with extremely high confidence (supplementary material Fig. S2) and has a solvation free energy gain upon dimerisation of –63.8 kcal/M (calculated on the PISA server http://www.ebi.ac.uk/msd-srv/prot_int/cgi-bin/piserver), which is similar to other BAR domain dimers (Masuda and Mochizuki, 2010). Furthermore, the high degree of conservation observed in the residues involved in dimerisation in both structures (i.e. the crystal structure of SNX9 and the theoretical model of *T. brucei* Vps5) is a good indication that TbVps5 might exist as a dimer with a dimeric structure close to that observed in the model (supplementary material Fig. S2). Together, these results strongly suggest the presence of BAR domains in trypanosomes.

Vps10 is a candidate universal retromer cargo, implicating an ancestral role in lysosomal hydrolase sorting

Vps10 is the most studied retromer cargo and is a transmembrane lysosomal hydrolase receptor orthologous to mammalian sortilins (Mari et al., 2008). Vps10 is relatively well retained, with expansions in *H. sapiens*, *D. rerio*, *N. vectensis*, *Monosiga brevicollis*, *S. cerevisiae*, *Rhizopus oryzae* and *Tetrahymena thermophila* (Fig. 1). The *S. cerevisiae*, *R. oryzae* and *T. thermophila* expansions are species-specific, whereas metazoan-specific expansions have generated several distinct metazoan sortilin-Vps10 families (Fig. 8).

Despite broad conservation, Vps10 was absent from several lineages, suggesting multiple secondary losses (Fig. 1). This is significant and suggests that retromer, although conserved, might be responsible for sorting distinct sets of cargo in different organisms. We therefore parsed the literature for all reported retromer cargo and performed comparative genomics of the 14 known cargo, as well as EHD1, a protein that has been shown to

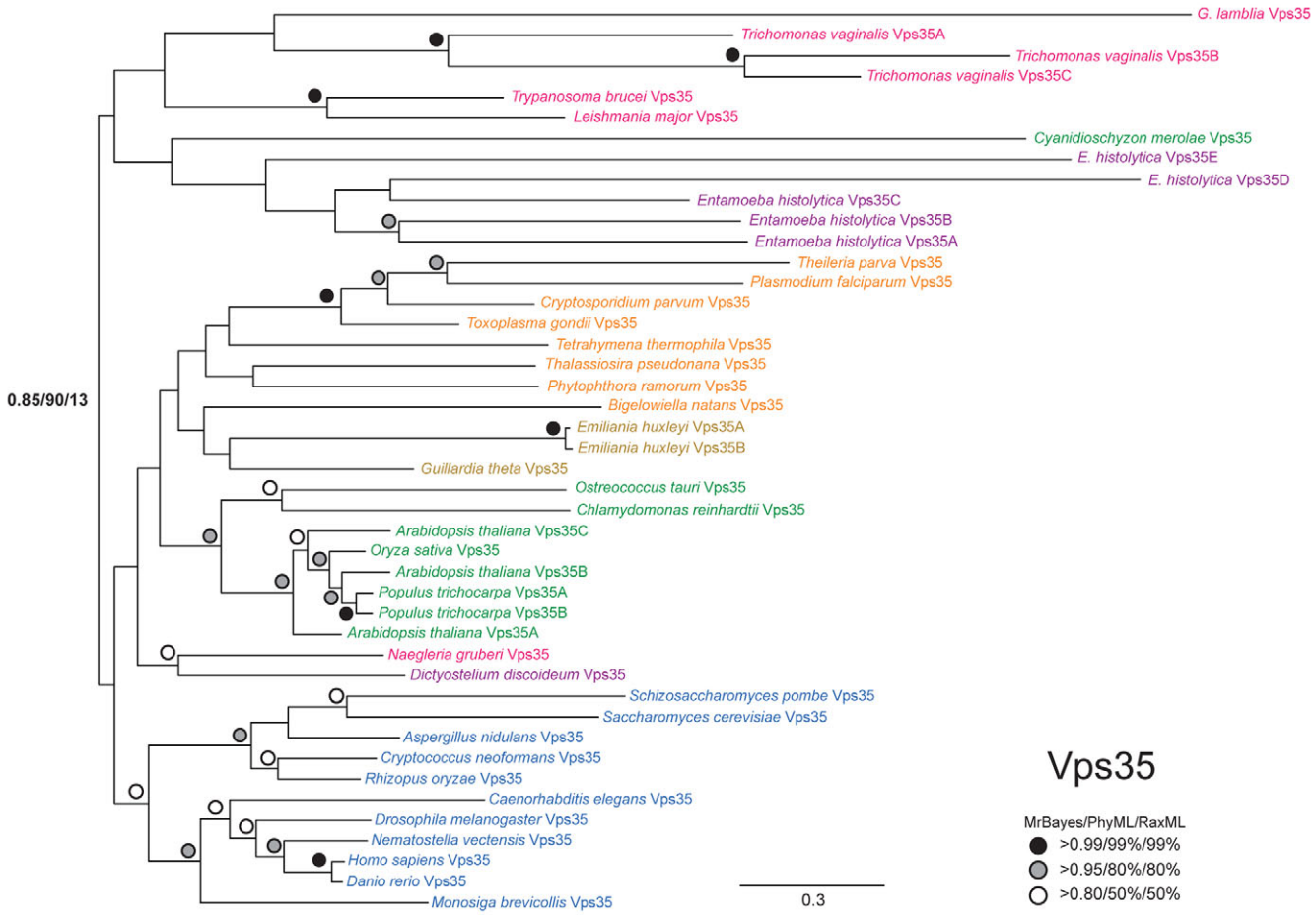

Fig. 4. Phylogenetic reconstruction of Vps35. The tree shown is the best Bayesian topology. Supergroup colour codes are as for Fig. 1; the numerical values at the nodes of the tree and symbols for highly supported nodes are as in Fig. 2.

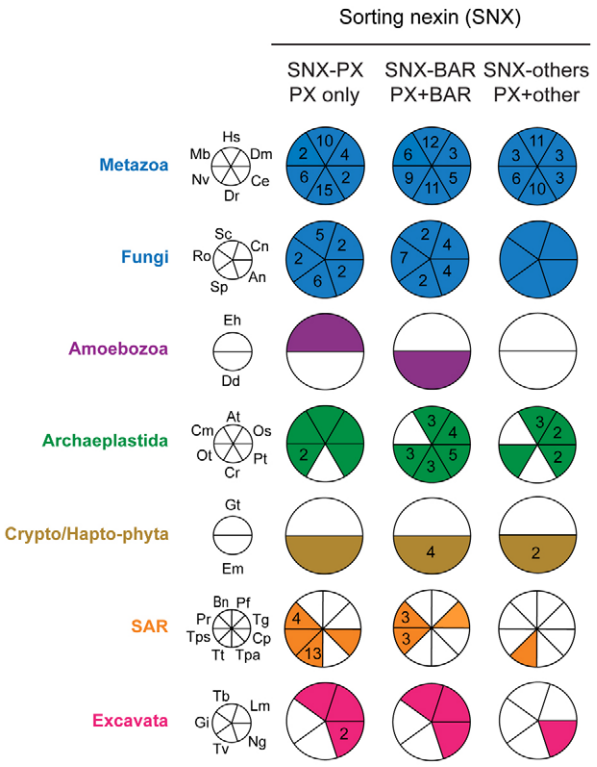

Fig. 5. Distribution of sorting nexins across the eukaryotes. Sorting nexins (SNX) can be classified on the basis of domain architecture: SNX-PX, PX domain only; SNX-BAR, PX and BAR domain; SNX-others, PX and an additional non-BAR domain. The assignment of the human sorting nexins into these three classes is according to Cullen (Cullen, 2008). Large taxon group colour codes, species names abbreviations and sector filling conventions are as in Fig. 1. Accession numbers are provided in supplementary material Table S1.

interact with retromer (Gokool et al., 2007). Most studies are from opisthokonts and indeed many of the reported cargo are specific to metazoans (Fig. 9). Several perform high-order functions in metazoan-specific signalling or immune defence (e.g. PIGR, EGFR and wntless). VSR1, originally identified in *A. thaliana* as a vacuolar sorting receptor (Yamazaki et al., 2008), is Archaeplastida restricted. However, we also found widely distributed cargo. Importantly, all species that lack Vps10 contain at least one putative alternative cargo (supplementary material Table S2).

EHD1, STE13 (DPAP), KEX2, FET3, FTR1 and CIMPR (Fig. 9) were all widely distributed among the eukaryotes. EHD1, an Eps15-homology domain protein family member, interacts with retromer and stabilises SNX1 tubules to facilitate endosome-to-Golgi retrieval (Gokool et al., 2007) but also participates in recycling from the endosome to the plasma membrane (Lin et al., 2001). Therefore, EHD1 conservation could be associated with either both or one of these recycling roles. Yeast STE13, a dipeptidyl aminopeptidase, and KEX2, a serine protease, are trans Golgi network (TGN) membrane proteins requiring retromer and SNX3 for retrieval from a prevacuolar compartment to the TGN (Nothwehr et al., 1999; Nothwehr and Hindes, 1997; Strochlic et al., 2007; Voos and Stevens, 1998). FET3 and FTR1, which comprise the yeast high-affinity iron transporter, are resident on the plasma membrane and require retromer and SNX3 for recycling to the plasma membrane (Strochlic et al., 2007).

CIMPR is classically responsible for lysosomal delivery of soluble molecules bearing the mannose 6-phosphate modification. Interestingly, we found some correlation between the presence of CIMPR and genes encoding the two enzymes required for mannose 6-phosphate modification, '*N*-acetylglucosamine-1-phosphotransferase subunits α/β precursor' (GNPTAB) and '*N*-acetylglucosamine-1-phosphodiester α' (NAGPA). *N. gruberi* was the only non-metazoan taxon that possessed both enzymes and the receptor. Fungi and amoebozoans possessing a CIMPR orthologue lacked one or both of GNPTAB and NAGPA, suggesting that CIMPR must have a mannose-6-phosphate-independent mechanism for recognition of cargo, consistent with data indicating that the *S. cerevisiae* CIMPR homologue retains a role in lysosomal targeting (Whyte and Munro, 2001), and suggesting that CIMPR might play a broader role than suspected in lysosomal delivery.

PEP12 is an endosomal SNARE (SynE) retrieved from prevacuolar endosomes to the TGN through action of retromer and SNX3 (Hettema et al., 2003). We recognised homologues of endosomal SNAREs in diverse eukaryotic taxa, but Pep12 is a yeast-specific endosomal SNARE with discrete localisation and function, even compared with that of other SynE paralogues (Pelham, 1999). This protein evolved convergently in eukaryotes (Dacks et al., 2008), so functionality with retromer cannot be presumed for other eukaryotic SynE homologues. Hence, we classified Pep12 as specific to yeast (Fig. 9).

Localisation and functional analysis of the retromer complex in *Trypanosoma brucei*

Our analysis establishes that retromer evolved early in the eukaryotic lineage and remains very well conserved. To elucidate functional conservation, we explored retromer location and activity in *T. brucei*. As an excavate, *T. brucei* is distantly related to mammals and yeast but possesses a well-characterised endomembrane system (Field and Carrington, 2009). *T. brucei* Vps5 mRNA expression (Tb09.211.4240) is strongly upregulated in the mammalian form (Koumandou et al., 2008) where endocytosis is also upregulated (Natesan et al., 2007); this is consistent with a role for *T. brucei* Vps5 in endocytic activity.

To investigate this further, quantitative real-time PCR (qRT-PCR) analysis was used to both confirm *T. brucei* Vps5 developmental regulation and examine expression of trypanosome retromer homologues Vps26 (Tb11.01.1770), Vps29 (Tb11.01.5900) and Vps35 (Tb10.70.5460) (supplementary material Fig. S3); all were upregulated in the mammalian stage. We used RNA interference (RNAi) knockdown against the *T. brucei* Vps5, Vps26 and Vps35 proteins to determine the importance of retromer component expression in cell viability. A severe proliferative defect was rapidly observed within 36 hours of RNAi induction for all three subunits (supplementary material Fig. S3), and it is probable that the loss of viability is due to a general defect in cellular processes rather than a specific cell cycle block (supplementary material Fig. S3).

To determine the location of trypanosome retromer, we generated epitope-tagged chimaeras of *T. brucei* Vps5 and *T. brucei* Vps26 with YFP and HA, respectively. Immunofluorescence indicated that both proteins exhibited diffuse cytoplasmic staining, with one or multiple distinct puncta located between the nucleus and kinetoplast (Fig. 10A), the region of the cell containing essentially all the endosomal apparatus (Field and Carrington, 2009). This suggests both organelle-targeted and cytoplasmic pools. Importantly, *T. brucei* Vps5 and Vps26 colocalised (Fig. 10A)

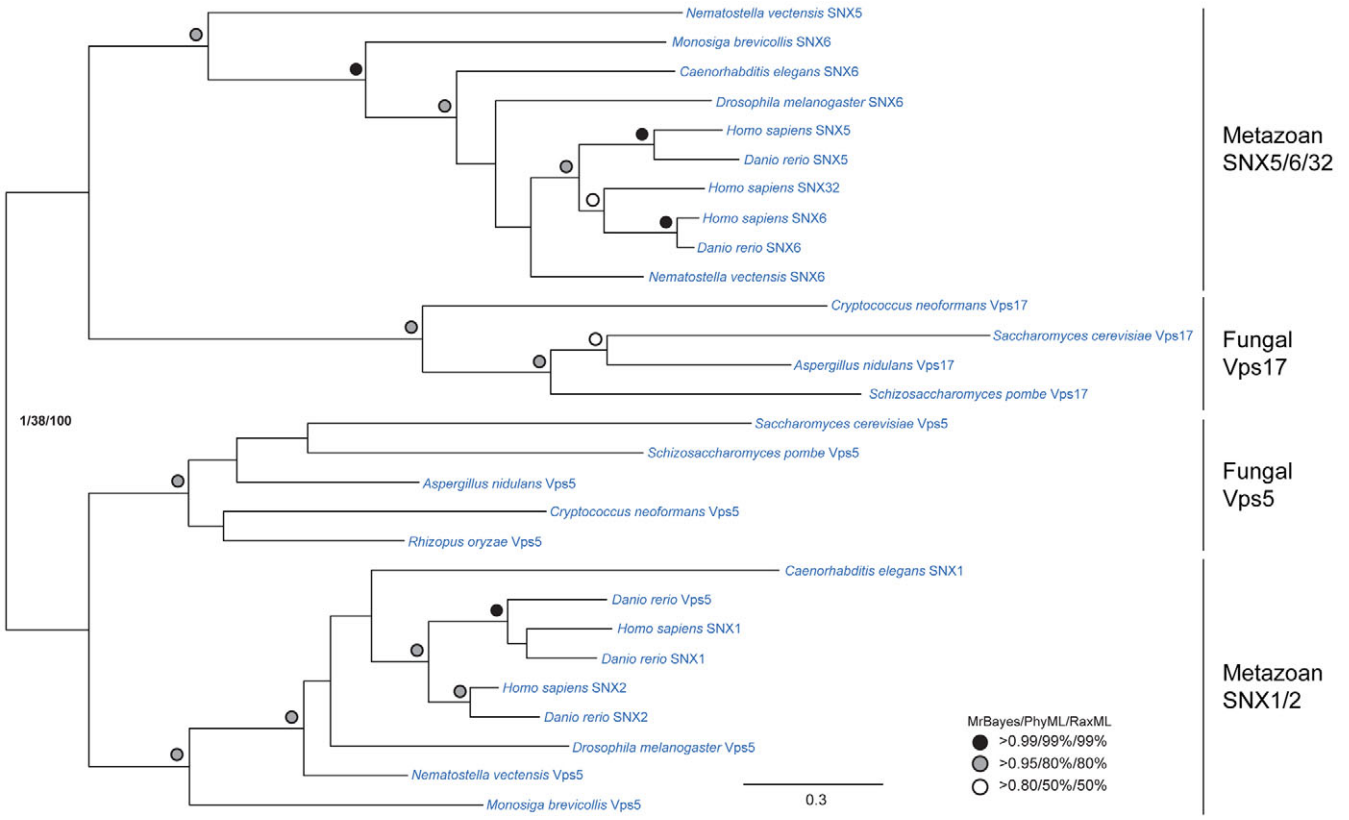

Fig. 6. Phylogenetic reconstruction of SNX-BAR sorting nexins in opisthokonts. The tree shown is the best Bayesian topology. Supergroup colour codes are as for Fig. 1; the numerical values at the nodes of the tree and symbols for highly supported nodes are as in Fig. 2. Four distinct clades can be observed: the metazoan SNX5, SNX6 and SNX32 (SNX5/6/32); fungal Vps17; fungal Vps5; and metazoan SNX1 and SNX2 (SNX1/2). Additionally, resolution of the central node separating SNX5/6/32 and Vps17, and Vps5 and SNX1/2, suggest that each pair shares a common ancestor.

consistent with the two proteins functioning in the same complex. Co-staining with several markers strongly suggested an endocytic location for the *T. brucei* Vps5 and Vps26 retromer subunits, in agreement with results from yeast and mammals. *T. brucei* Vps26 partially colocalised with the clathrin heavy chain (CLH), Rab5A, the recycling endosome (Rab11) and epsinR (Fig. 10B). *T. brucei* Vps26 was proximal to Vps28, which marks the multivesicular body (MVB), and to the lysosomal marker p67, whereas no colocalisation was observed with a GRASP Golgi marker (Fig. 10B). Overall these data indicate an endosomal location.

To explore further retromer function in *T. brucei*, we examined the effects of RNAi against retromer components on lysosomal and Golgi markers. We found a modest but significant increase in lysosomal marker p67 expression, as measured by immunofluorescence after RNAi knockdown of *T. brucei* Vps5, Vps26 or Vps35 (Fig. 11A,B). This might represent a modest increase to lysosomal traffic through a block of trafficking from the MVB due to the loss of retromer, as seen in yeast and mammalian cells (Raymond et al., 1992). Furthermore, we found that RNAi knockdown of *T. brucei* Vps5 resulted in a modest but significant decrease to intracellular levels of ISG75 (Fig. 11C), a transmembrane protein that traffics through the endosomal system and undergoes ubiquitin-dependent degradation (Chung et al., 2008; Leung et al., 2008). The decrease in ISG75 endosome-associated staining is at least in part due to accelerated turnover, and cannot simply be attributed to defective uptake, as *T. brucei* Vps5 RNAi leads to more rapid degradation (Fig. 11C). Although the precise itinerary of ISG75 is not yet known, these data clearly indicate that retromer participates in trafficking of surface proteins en route through the endosomal system. Finally, a well documented effect of retromer in mammalian cells is fragmentation of the Golgi complex on silencing Vps26 (Seaman, 2004); a very similar effect was found in trypanosomes, with dispersal of the Golgi marker GRASP upon *T. brucei* Vps26 knockdown (Fig. 11D). Together the locations and effects of retromer subunit knockdowns suggest functional homology between trypanosome and mammalian and yeast retromer.

Discussion

The retromer complex participates in intracellular retrograde transport from the endosome to the Golgi. It functions to recycle receptors that traffic proteins to the endosome and the lysosome, and to recycle proteins and receptors that traffic through the endocytic system but that are not destined for destruction at the lysosome. Owing to this central role in intracellular trafficking, normal function of the retromer is vital for many recycling processes, and loss or malfunction of retromer is associated with various pathological states due to protein mistargeting. Retromer might have a role analogous to COPI, COPII and clathrin vesicle coats in selecting cargo and mediating trafficking between specific organelles. Given that these other vesicle coats are well conserved throughout the eukaryotes, we examined the evolution of retromer.

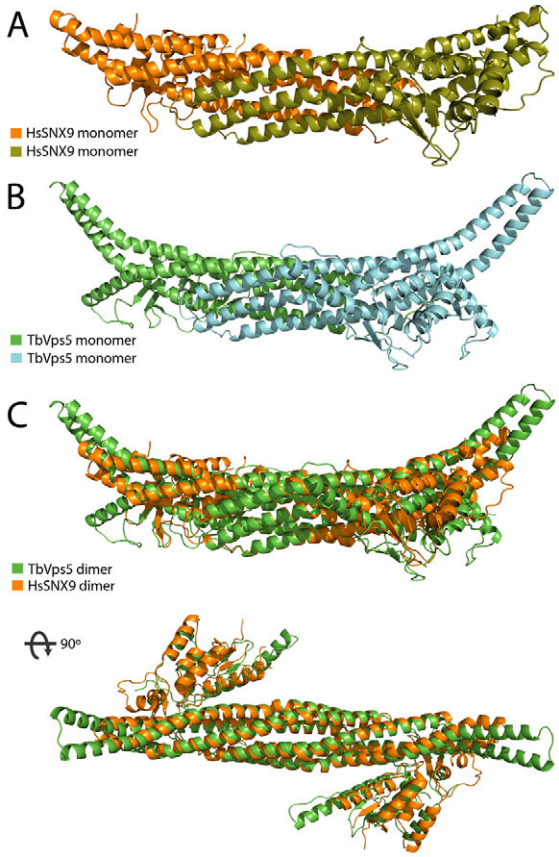

Fig. 7. Molecular model of *T. brucei* Vps5 based on the structure of human SNX9. (**A**) Structure of human sorting nexin 9 (PDB ID: 2RAI) (Pylypenko et al., 2007). Two SNX9 monomers are shown, coloured orange and khaki. (**B**) Structure of the *T. brucei* Vps5 dimer modelled on human SNX9. The two monomers of *T. brucei* Vps5 are green and cyan. The dimer adopts a curved topolology characteristic of BAR domain dimers, with extended helices at the ends of the helix bundles compared with those in SNX9. The predicted structure has very high confidence (supplementary material Fig. S2). (**C**) Superimposed structures for the human SNX9 dimer (orange) and the *T. brucei* Vps5 dimer (green), in the same orientation as A and B and rotated 90° along the *x*-axis, showing the concave face of the curved structure with the PX domains extending above and below. See also supplementary material Movies 1 and 2.

We found that the retromer complex is extremely well conserved throughout eukaryotes. Specifically, the cargo-selective subcomplex, composed of Vps26, Vps29 and Vps35, was present in all eukaryotes examined, indicative of an ancient origin before the LECA. This level of conservation for Vps26, Vps29 and Vps35 among the different eukaryotic lineages examined is exceptional. Comparative genomics revealed evidence of species-specific expansions for Vps26, Vps29 and Vps35, especially in Metazoa, Archaeplastida and *T. vaginalis*. Evidence for a tissue-specific function for Vps26 isoforms in mouse, as well as distinct intracellular locations (Kerr et al., 2005; Kim et al., 2008), suggests that these expansions could result in diversification of retromer function. The membrane-deforming subcomplex, composed of two sorting nexins, was also highly conserved, although there was more variability within sorting nexin orthologues than for the other retromer components. Additionally, certain species lacked recognisable sorting nexins altogether (*G. theta*, *P. falciparum*, *T. parva*, *T. vaginalis* and *G. intestinalis*). These results argue for an ancient origin of the whole retromer complex, although they suggest flexibility in the sorting nexin dimer, and raise interesting questions as to the function of retromer in organisms lacking a typical membrane-deforming subcomplex. Although PX-domain-containing proteins have been reported for *P. falciparum* and *G. intestinalis* (Banerjee et al., 2010), these do not look like sorting nexins by reverse BLAST, apart from a putative example in *Giardia* (GL50803_16548). Recent evidence suggests that endosome recruitment of the cargo-selective retromer subcomplex might involve factors other than the sorting nexins, notably Rab7 (Nakada-Tsukui et al., 2005; Rojas et al., 2008; Seaman et al., 2009). Rab7 is conserved in all species studied herein that lack sorting nexins, except for *G. intestinalis*, which might be due to either high sequence divergence or to the highly unusual nature of endocytic organelles in *Giardia* (Abodeely et al., 2009).

Given the divergence of sorting nexin homologues within the eukaryotes, and the fact that *Dictyostelium*, *Toxoplasma* and the kinetoplastids only contain one recognisable sorting nexin homologue with a BAR domain, we constructed a model of the dimer of the *T. brucei* protein to gain more information about its putative function. Indeed, the model agrees with the hypothesis that the protein can dimerise and aid in membrane deformation as part of the retromer complex. Although dimerisation of *T. brucei* Vps5 in vivo needs to be verified experimentally, the presence of the BAR domain in kinetoplastids indicates that the ancestor of the Excavata probably also possessed BAR-domain proteins and, together with the presence of BAR domains in opisthokonts, is compelling evidence for an ancient origin.

The exceptional conservation of retromer, including BAR-domain sorting nexins, among the eukaryotes suggests that retromer constitutes a third membrane deforming complex known to be conserved and ancient within the eukaryotic trafficking system, after the ESCRTs and protocoatomer (DeGrasse et al., 2009; Leung et al., 2008). The protocoatomer hypothesis suggests common ancestry for the nuclear pore complex and many vesicle coat complexes, as they share an N-terminal β-propeller and a C-terminal α-solenoid fold (DeGrasse et al., 2009; Devos et al., 2004). Interestingly, Vps26 is an exclusively β-protein resembling β-arrestin, whereas Vps35 forms a horseshoe-shaped right-handed α-helical solenoid, resembling other important coated vesicle proteins, for example the helical repeat regions of the heavy chain of clathrin and the Sec13–Sec31 unit of COPII (Hierro et al., 2007). This indicates a potentially similar architecture for retromer and protocoatomer, which might result from distant, and as yet undetected, homology. However, further evidence would be required to substantiate this hypothesis.

Retromer functions in trafficking of specific membrane receptors and many other cargos. Therefore, given the ancient origin of retromer, conservation of retromer cargo proteins might also be expected throughout the eukaryotes. Our analysis indeed indicates very good conservation of Vps10, the sorting receptor for lysosomal hydrolases, among all eukaryotic lineages, as well as expansion of the sortilin family early in the evolution of the Metazoa. However, secondary loss of Vps10-sortilin is also very common, which prompted examination of additional retromer cargo proteins, mostly identified from studies in yeast and mammals. Our results indicate two cohorts of conserved and lineage-specific cargo molecules. All the well-conserved cargo proteins are involved in diverse cellular processes and/or intracellular trafficking routes (e.g. they act as Golgi peptidases, in recycling from the plasma membrane or in

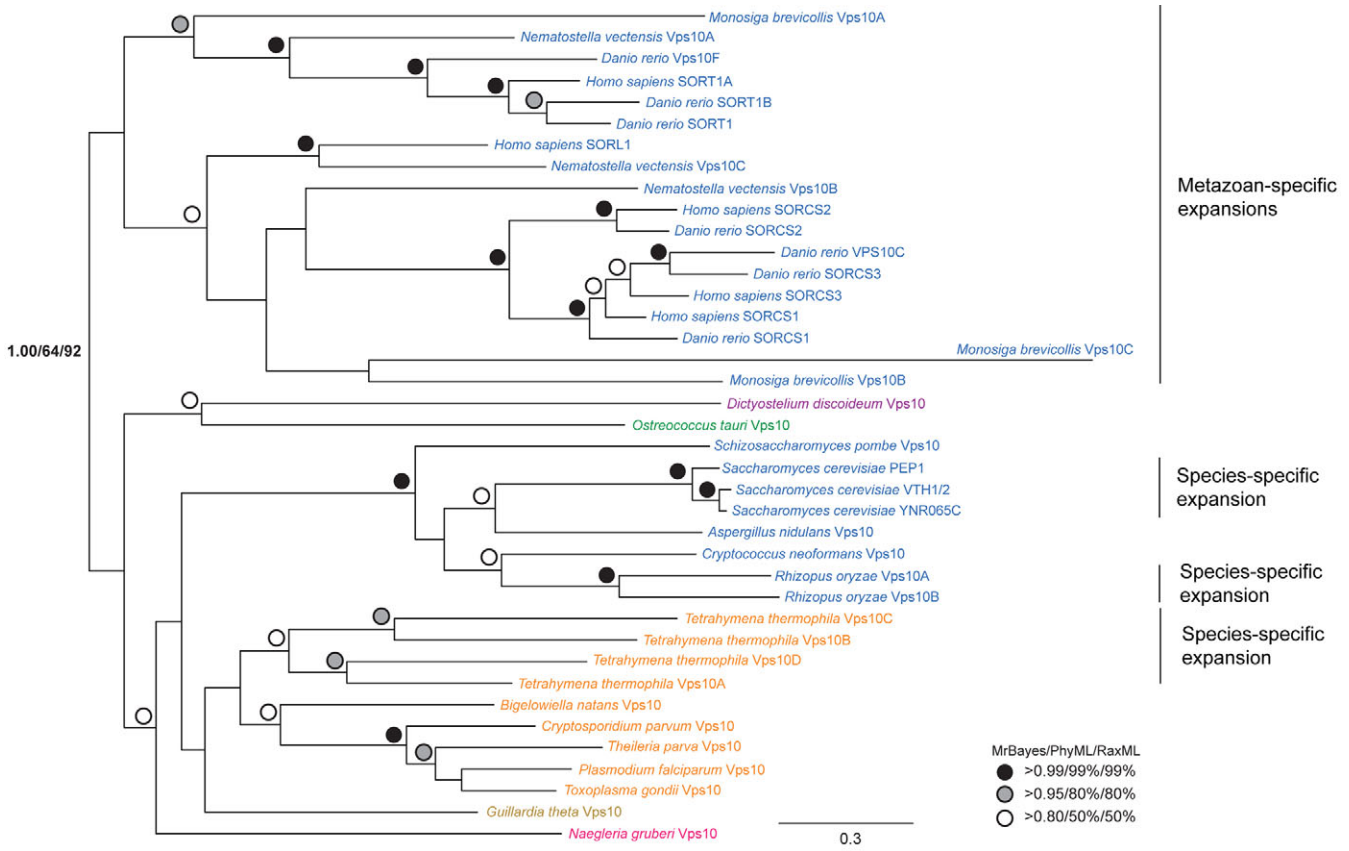

Fig. 8. Phylogenetic reconstruction of Vps10. The tree shown is the best Bayesian topology. Supergroup colour codes are as for Fig. 1; the numerical values at the nodes of the tree and symbols for highly supported nodes are as in Fig. 2. Species-specific expansions are seen for *S. cerevisiae*, *R. oryzae* and *T. thermophila*, and multiple further expansions originating before individual speciation events are evident in the Metazoa.

iron homeostasis). Importantly, all species examined in which Vps10-sortilin had been lost, contained at least one putative alternative retromer cargo (supplementary material Table S2). This result, along with the variety of retromer cargo reported in the Metazoa, suggest flexibility of retromer to recognise and traffic different cargo molecules, typical of vesicle coats, whereas lineage-specific cargo proteins are not uncommon (e.g. VSR1 in plants and EGFR in Metazoa).

To complement the comparative genomics and phylogenetics analysis of retromer, we examined the localisation and function of the complex in *T. brucei*. *T. brucei* has a complete, yet simplified, trafficking system, which has been extensively studied (Field and Carrington, 2009). *T. brucei* Vps5 is strongly upregulated in the mammalian infective form, compared with its expression in the insect proliferative stage, and thus could be important for pathogenesis (Koumandou et al., 2008). Indeed, qRT-PCR analysis confirmed that all components of retromer identified by comparative genomics in *T. brucei* are upregulated in the mammalian form; this might be related to the more active lysosomal delivery route in the procyclic stage, whereas in the bloodstream stage recycling is the major trafficking route in terms of flux (Field et al., 2007b). Retromer might contribute here, rescuing proteins before lysosomal delivery. RNAi knockdown of *T. brucei* Vps5, Vps26 and Vps35 led to severe proliferative defects, suggesting that the retromer complex is vital in trypanosomes. Immunofluorescence microscopy of epitope-tagged versions of *T. brucei* Vps5 and Vps26 proteins indicated that they colocalise and are present at endosomal compartments. Proximity to markers for the MVB and lysosome indicate a position close to the MVB and the lysosome, with no steady-state or permanent presence at the Golgi complex. Knockdown of retromer components had a moderate effect on p67 (a LAMP analogue) intensity and location. Furthermore, RNAi knockdown of *T. brucei* Vps5 resulted in a decrease in intracellular levels of ISG75, in part due to increased turnover, potentially due to retromer-mediated defects in endosomal recycling pathways. Finally, prolonged RNAi knockdown of *T. brucei* Vps26 leds to dispersal of the immunofluorescence signal for the Golgi marker GRASP, similar to the fragmentation of Golgi membranes seen in mammalian cells after Vps26 knockdown (Seaman, 2004). Although the precise effects of retromer knockdown remain to be determined, the data indicate a rather similar phenotype in this organism when compared with that in conventional model systems.

Overall, our results point to an ancient origin for retromer and Vps10, and imply an ancestral role for retromer in lysosomal targeting. However, this ancient complex manifests the potential for much functional flexibility. Moreover, retromer appears to have a conserved endosomal localisation and function in *T. brucei*, lending further support to the comparative genomics evidence for a conserved and ancient function in all eukaryotes. Despite the possibility of homology with the protocoatomer complexes, retromer and the BAR domain do appear to be yet another novel membrane-deformation strategy already evolved before the LECA, over one and a half billion years ago.

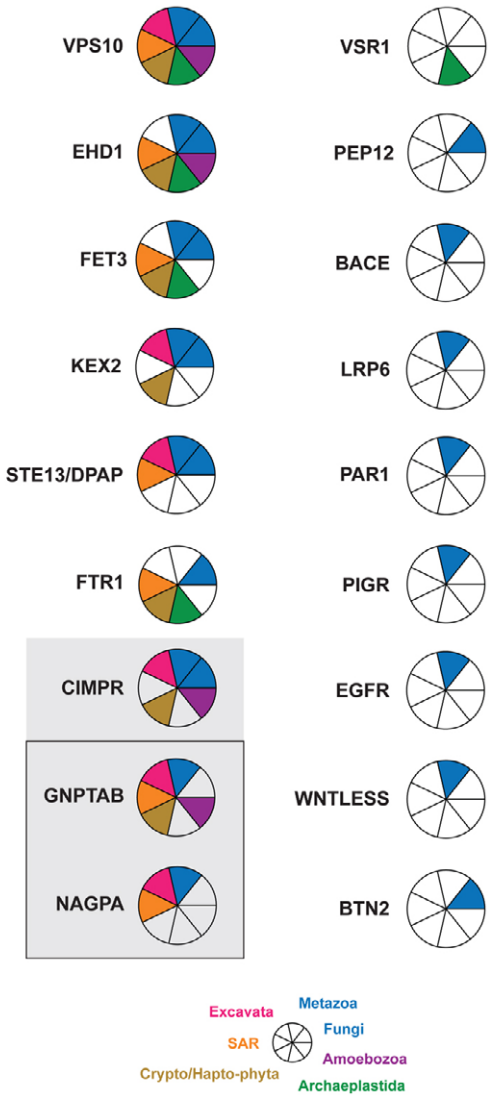

Fig. 9. Distribution of proteins previously identified as interacting with retromer across the range of eukaryotic lineages. Large taxon groupings are colour coded (key at bottom). Filled sectors indicate the presence of a protein in the respective supergroup, on the basis of a clear reverse BLAST; white sectors indicate that the protein was not found. Accession numbers are in supplementary material Table S2. Protein name abbreviations and selected references relating to their interaction with retromer are as follows: Vps10, vacuolar protein sorting 10, similar to mammalian sortilins (Seaman et al., 1997); EHD1, Eps15-homology-domain-containing protein-1 (Gokool et al., 2007); STE13 (DPAP), dipeptydyl aminopeptidase (Nothwehr et al., 1999; Nothwehr et al., 2000); KEX2, killer expression defective 2 serine protease (Nothwehr and Hindes, 1997); FET3, ferrous transport 3 (Strochlic et al., 2007); FTR1, Fe transporter 1, forms part of the yeast reductive iron transporter with Fet3 (Strochlic et al., 2007), PEP12, carboxypeptidase-Y-deficient 12 (Hettema et al., 2003); CI-MPR, cation-independent mannose 6-phosphate receptor (Arighi et al., 2004; Seaman, 2004); VSR1, vacuolar sorting receptor 1 (Yamazaki et al., 2008); BACE, β-secretase, also known as memapsin 2 (He et al., 2005); LRP6, lipoprotein-receptor-related protein 6 (George et al., 2007); PAR1, protease-activated receptor-1 (Gullapalli et al., 2006); PIGR, polymeric immunoglobulin receptor (Verges et al., 2004; Verges et al., 2007); EGFR, epidermal growth factor receptor (Gullapalli et al., 2004); wntless, G-protein-coupled receptor 177 or Wnt receptor (Eaton, 2008); BTN2, Batten disease protein 2 (Kama et al., 2007). Also included are results of searches for GNPTAB and NAGPA, enzymes required for synthesis of mannose 6-phosphate (boxed).

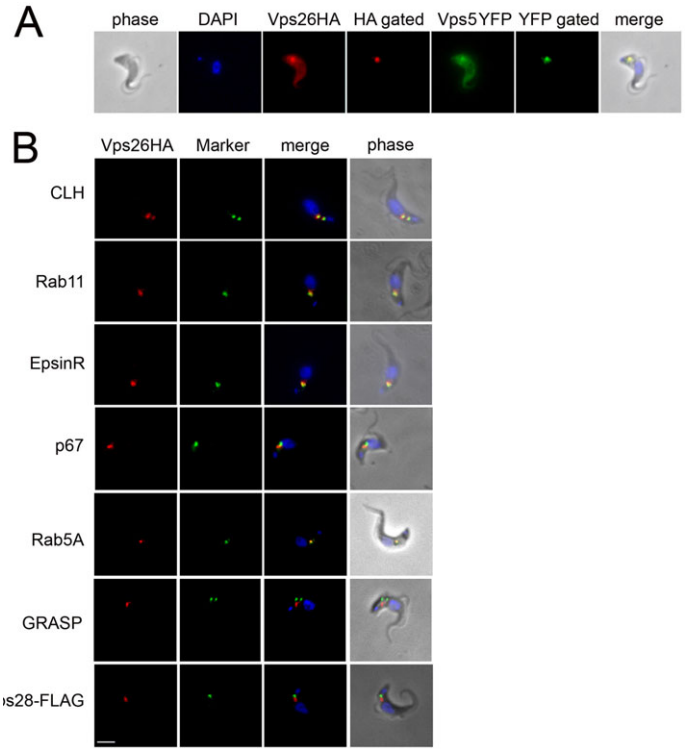

Fig. 10. *T. brucei* Vps26 and *T. brucei* Vps5 localise to the endocytic system. Retromer complex subunits *T. brucei* Vps26 and *T. brucei* Vps5 were ectopically expressed and labelled with HA and YFP, respectively. Their intracellular location was determined by immunofluorescence, using a mouse anti-HA antibody (red) and a FITC-conjugated secondary antibody (green), and cells were counterstained with DAPI for DNA (blue). (**A**) Both *T. brucei* Vps26 and *T. brucei* Vps5 showed diffuse cytoplasmic staining, as well as one or two distinct puncta; the 'gated' panels show images upon data processing to emphasise only the puncta. Similar gating was used for images in B. Both proteins localise to the posterior of the cell, between the nucleus and cytoplasm, which corresponds to the location of the endocytic apparatus. (**B**) Colocalisation of *T. brucei* Vps26–HA with a repertoire of endosomal markers [*T. brucei* clathrin heavy chain (CLH), Rab5A, Rab11, epsinR, GRASP, p67 and Vps28]. Scale bar: 2 µm.

Materials and Methods

Taxonomic homology survey

Taxon sampling of 34 species, representing all eukaryotic supergroups, was used (Adl et al., 2005). Where possible, two or more taxa were included from each supergroup to facilitate detection of secondary loss and to minimise detection failure from species-specific divergence. Details of databases are given in supplementary material Table S1. *B. natans* and *G. theta* retromer components were assembled from sequence reads produced from preliminary assemblies from the Joint Genome Institute. Initial queries for Vps5, Vps10, Vps17, Vps26, Vps29 and Vps35 typically used *H. sapiens* or *S. cerevisiae* predicted proteins and BLAST (Altschul et al., 1997) using the BLOSUM62 amino acid matrix with manual cutoff. Where initial searches failed, queries from closely related taxa to the subject were used. If this also failed, HMMer was used with a template composed of the entire set of proteins for each family. All recovered sequences were subjected to reverse BLAST against the original genome (*H. sapiens* or *S. cerevisiae*) and the nr database for confirmation of orthology. A candidate orthologue was considered retrieved if reverse BLAST recovered the original query or annotated orthologues from other species within the top five hits. Sequences were also parsed through the NCBI conserved domain database (CDDB) using default parameters and analysed for the presence of domains. Furthermore, candidates were subjected to phylogeny to confirm orthology. Failure to complete these tests resulted in an assignment of 'not found'. For SNX proteins, an HMM profile of all 33 human sorting nexins was constructed and used to search by HMMer, with individual hits verified by reverse BLAST.

For cargo (excluding Vps10) an automated BioPerl script was used to retrieve BLAST results; a homologue was recorded only if reverse BLASTs back to the original query had an E-value<e^{-5}. Yeast, human and *Arabidopsis* proteins used as the original queries are highlighted in supplementary material Table S2. In addition,

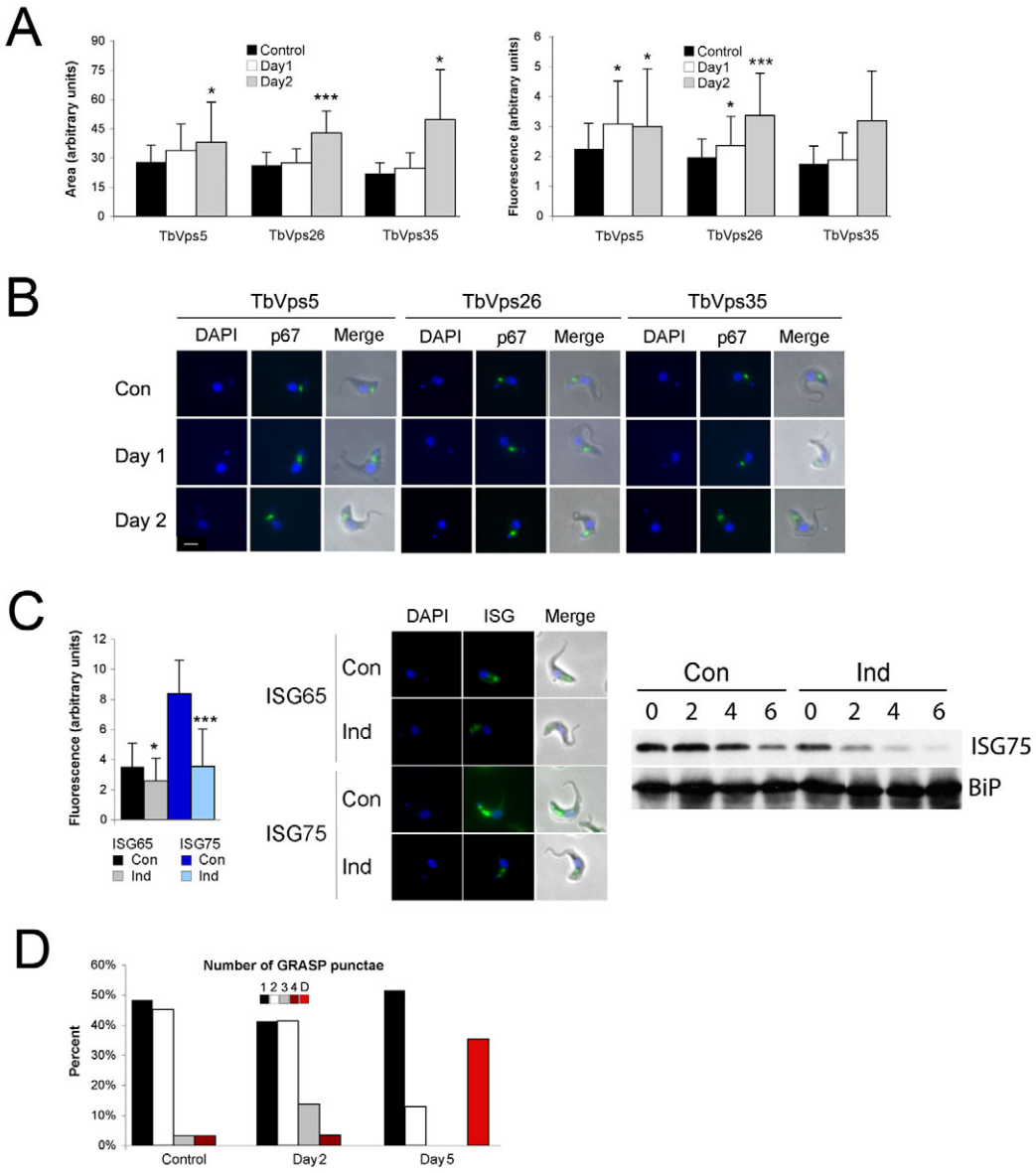

Fig. 11. Knockdown of retromer components in *T. brucei* affects the lysosome, the Golgi complex and endosomal trafficking. (**A**) Staining for lysosomal marker p67 was quantified by immunofluorescence after RNAi knockdown of *T. brucei* Vps5, *T. brucei* Vps26 and *T. brucei* Vps35. A modest (~30–50%), but significant, increase in both the p67 total signal and area was seen after knockdown of each retromer subunit at 2 days after induction in 1N1K cells. The data are mean+s.d. for at least 30 cells per sample (* $P<0.05$; ** $P<0.005$; *** $P<0.0005$ as measured by Welch's unpaired *t*-tests for the induced compared with the non-induced cell lines). (**B**) Representative images for p67 immunofluorescence in control and tetracycline-induced RNAi lines for *T. brucei* Vps5, *T. brucei* Vps26 and *T. brucei* Vps35, at 1 and 2 days post induction. Scale bar: 2 µm. (**C**) Left-hand panel: staining for the trans-membrane proteins ISG65 and ISG75, which traffic through the endosomal system, was measured by immunofluorescence after RNAi knockdown of *T. brucei* Vps5. A modest (20–50%), but significant, decrease in the ISG75 total signal and area is seen after knockdown at 2 days after induction in 1N1K cells. Error bars and significance values are as in A. Centre panel: representative images for ISG65 and ISG75 immunofluorescence in control and tetracycline-induced RNAi lines for *T. brucei* Vps5 at 2 days post induction. Right-hand panel: ISG75 is destabilised after RNAi knockdown of *T. brucei* Vps5, as seen by western blotting of whole cell lysates, after treatment with cycloheximide. *T. brucei* BiP was used as a loading control. (**D**) Morphology of the Golgi complex monitored by anti-GRASP antibody immunofluorescence after RNAi knockdown of *T. brucei* Vps26. Non-induced cells have one or two distinct GRASP spots, where an increased number of spots is indicative of Golgi disruption. A significant effect is seen at 5 days post induction, where 40% of 1N1K cells have a weak and dispersed GRASP signal (D) instead of distinct spots.

homology searches were performed manually. Homologues were recorded only if they retrieved the original query or a named version thereof with an E-value<0.05. However, in some cases, more stringent criteria were used; STE13 (DPAP) candidates needed to possess both the dipeptidyl peptidase IV N-terminal region (DPPIV_N) and the prolyl oligopeptidase (peptidase_S9) Pfam domains. Additionally, EHD1 needed to possess the Era-like and EH domains (Conserved Domain Database). For each cargo protein, HMM profiles were constructed using homologues retrieved by BLAST with the lowest E-value from each organism. These were used to search any proteome in which BLAST did not recover a homologue. HMMer was used to search for EGFR homologues outside of opisthokonts.

Alignments and phylogenetic reconstructions

Alignments (available upon request) were created using MUSCLE (Edgar, 2004). Only unambiguous homologous regions were retained for phylogenetic analysis. Details of data sets are in supplementary material Tables S1 and S2. ProtTest (Abascal et al., 2005) was used to estimate the appropriate model of sequence

evolution. Phylogenetic analysis was performed by three separate methods. To obtain the Bayesian tree topology and posterior probability values, the program MrBayes version 3.1.2 was used (Ronquist and Huelsenbeck, 2003). Analyses were run for 1–5($\times 10^6$) generations, removing all trees before a plateau established by graphical estimation. All calculations were checked for convergence and had a splits frequency of <0.1. Maximum-likelihood (ML) analysis was performed using PhyML (Guindon and Gascuel, 2003) and RAxML (Stamatakis, 2006) with 100 bootstrap replicates. Nodes with better than 0.95 posterior probability and 80% bootstrap support were considered robust, and nodes with better than 0.80 posterior probability and 50% bootstrap support are shown.

Plasmid construction

Primers for amplification of an RNAi target were designed using RNAit (Redmond et al., 2003). RNAi fragments were PCR amplified using Taq DNA polymerase with gene-specific primers (TbVPS35-RNAi-F, 5′-TACCAGGTGAAGGCGGTTAC-3′; TbVPS35-RNAi-R, 5′-CAGCATACTTTCCCAACCGT-3′; TbVPS26-RNAi-F, 5′-ATACTCAGCCGGACGCTCTA-3′; TbVPS26-RNAi-R, 5′-TTGCCGTCAG-CAGTTATCAG-3′; TbVps5-RNAi-F, 5′-CCTGCATGAATTTGGTGTTG-3′; TbVps5-RNAi-R, 5′-TCTGCAGGTCAGCAAACATC-3′) and cloned into the RNAi vector p2T7^{TAblue}, linearised with *Eam*1105I. Trypanosome orthologues of Vps5 and Vps26 were amplified from trypanosome 427 genomic DNA using Vent DNA polymerase (New England BioLabs) with primers (TbVps5-YFP-F, 5′-CTG-CAAGCTTCTGAAAATGTCTTTGAGTTC-3′; TbVps5-YFP-R, 5′-GACTGGATC-CCTAATCGTCATCAATCAAAT-3′; TbVPS26-CHA-F, 5′-TACTAAGCTTAT-GTTGGAGCGGGAGCGGCC-3′; TbVPS26-CHA-R, 5′-AGTAGGGCCCTGCAT-GAGATGTTTCACCCG-3′). PCR products for *T. brucei* Vps26 were cloned into the expression vector pXS5, containing sequence for a C-terminal HA-epitope tag, using *Hin*dIII and *Apa*I. PCR products for *T. brucei* Vps5 were cloned into the vector pHD1034, containing sequence for an N-terminal YFP-epitope tag, using *Hin*dIII and *Bam*HI. All constructs were verified by standard sequencing methods (Geneservice) before introduction into trypanosomes, and expression was verified by western blotting where appropriate. The TbVps28-FLAG vector was a gift from Ka-Fai Leung (Cambridge, UK) (Leung et al., 2008).

Transfection of the bloodstream form of *T. brucei*

Culturing of the bloodstream form of *T. brucei* was as described previously (Leung et al., 2008). Cells (3×10^7) were harvested at 800 ***g*** for 10 minutes at 4°C, and an Amaxa nucleofector (Burkard et al., 2007) was used for transfection with 10–25 μg of linearised plasmid. Cells were transferred into HMI-9 complete medium and allowed to recover at 37°C for 6 hours. Antibiotic(s) was added for selection, and cells were subdivided into a 24-well plate. Clones were selected for hygromycin resistance at ~5 days post-transfection. Induction of RNAi and growth analysis were as described previously (Leung et al., 2008).

Quantitative real-time PCR

RNA extraction and qRT-PCR analysis were as previously described (Koumandou et al., 2008). Primers were: TbVps5-RTF,5′-AGCGTTGGTCAAGTGCTTTC-3′; TbVps5-RTR, 5′-CCCTCCCATGCAGTCATATC-3′; TbVPS26-RTF, 5′-TG-TACGTTCTCCGTGTGGTC-3′; TbVPS26-RTR, TAGAGCGTCCGGCTGAGTAT-3′; TbVPS29-RTF, 5′-GTTTACACCTGGCCGCATAC-3′; TbVPS29-RTR, 5′-CGAGTCAAACTCACCCTTGG-3′; TbVPS35-RTF, 5′-GGTGATGGCAAGGGT-GTATT-3′; TbVPS35-RTR, 5′-CGTAGATCACCTCGGAAAGC-3′.

Immunofluorescence

Preparation of samples, and acquisition and processing of images was as described previously (Leung et al., 2008). Antibodies were used at the following dilutions: mouse and rabbit anti-HA epitope antibody (both from Santa Cruz Biotechnology) at 1:1000, rabbit anti-YFP antibody at 1:500, rabbit anti-ISG65 and rabbit anti-ISG75 antibodies (from Mark Carrington, Cambridge, UK) at 1:1000, rabbit anti-Rab5A antibody at 1:200, rabbit anti-Rab11 antibody at 1:400, mouse anti-p67 antibody (from James Bangs, Madison, WI) at 1:1000, rabbit anti-GRASP antibody at 1:500, rabbit anti-clathrin antibody at 1:250 and rabbit antibody against *T. brucei* EpsinR at 1:500. Secondary antibodies were Oregon-Green-488-conjugated anti-(mouse IgG) (Molecular Probes) at 1:1000 and Alexa-Fluor-568-conjugated anti-(rabbit IgG) (Invitrogen) at 1:1000. Cells were examined on a Nikon Eclipse E600 epifluorescence microscope fitted with optically matched filter blocks and a Hamamatsu ORCA CCD camera. Images were captured using METAMORPH software (Universal Imaging) and processed using Adobe Photoshop. Quantification of the areas of fluorescent spots and integration was performed using the raw data, from identical exposures, as appropriate, and the Metamorph Region Measurements function. Welch's unpaired *t*-test (GraphPad software) was used to check the significance.

Protein turnover

Protein synthesis was blocked by the addition of cycloheximide (100 μg/ml), and samples were analysed by western blotting, as described previously (Leung et al., 2008). Antibodies were used at the following dilutions: rabbit anti-ISG65 and rabbit ISG75 antibodies at 1:5000, rabbit anti-BiP antibody at 1:10,000, and horseradish-peroxidase-conjugated anti-(rabbit IgG) and anti-(mouse IgG) (A0545; Sigma) at 1:10,000. Densitometry quantification was achieved using ImageJ (NIH).

Structural model of *T. brucei* Vps5

The SWISS-MODEL Workspace automated homology-modelling server (http://swissmodel.expasy.org) (Arnold et al., 2006) was used to search for homologous structures to *T. brucei* Vps5 (Tb09.211.4240). The phosphoinositide-binding Phox homology (PX) and the Bin-amphiphysin-Rvs (BAR) domains of human sorting nexin 9 (SNX9) (Pylypenko et al., 2007) were selected as appropriate homologues of *T. brucei* Vps5. Amino acid sequence and three-dimensional structures were obtained from the Protein Data Bank (http://www.rcsb.org/pdb/) [PDB IDs: 2RAJ, (SNX9 monomer) and 2RAI (dimer)]. Initial amino acid sequence alignment between *T. brucei* Vps5 and the template (SNX9) was performed using FUGUE (Shi et al., 2001).

Theoretical models of the structure of the *T. brucei* Vps5 dimer were obtained by MODELLER (Sali and Blundell, 1993). MODELLER generates protein structures by satisfaction of spatial restraints with simultaneous optimisation of CHARMM energies, conjugate gradients and molecular dynamics with simulated annealing. Comparative models were validated with PROCHEK (Laskowski et al., 1993) and WHAT_CHECK (Hooft et al., 1996), which evaluates geometry of the structure of the protein, VERIFY3D (Luthy et al., 1992), which reports amino acid environment, and JOY (Mizuguchi et al., 1998), for comparison of the modelled structure with homologous proteins. Alignments were manually modified when models were unsatisfactory, and the modelling and validation processes were repeated until models with good geometry and conformation were obtained.

This study was supported by the Wellcome Trust (to M.C.F.). We are indebted to CAMPOD for equipment funds, EMBO and the Biochemical Society (travel grants to V.L.K.) and the NSERC of Canada (to J.B.D.). We thank the various genome projects that make their data publicly available and especially J. M. Archibald, M. W. Gray, P. J. Keeling, G. I. McFadden and C. E. Lane for access to preliminary data from *Guillardia theta* and *Bigelowiella natans*, produced by the Joint Genome Institute (http://www.jgi.doe.gov/). Work conducted by the U.S. Department of Energy JGI is supported by the Office of Science of the U.S. Department of Energy (DE-AC02-05CH11231). We acknowledge CamGrid, on which some of these analyses were performed, Amanda O'Reilly, for BioPerl, and Shona Wilson for statistical advice. We thank Mark Carrington for the antibodies against ISG65 and ISG75, James Bangs for the anti-p67 antibody and Graham Warren for the anti-TbGRASP antibody. Deposited in PMC for release after 6 months.

Supplementary material available online at
http://jcs.biologists.org/cgi/content/full/124/9/1496/DC1

References

Abascal, F., Zardoya, R. and Posada, D. (2005). ProtTest: selection of best-fit models of protein evolution. *Bioinformatics* **21**, 2104-2105.

Abodeely, M., DuBois, K. N., Hehl, A., Stefanic, S., Sajid, M., DeSouza, W., Attias, M., Engel, J. C., Hsieh, I., Fetter, R. D. et al. (2009). A contiguous compartment functions as endoplasmic reticulum and endosome/lysosome in *Giardia lamblia*. *Eukaryot. Cell* **8**, 1665-1676.

Adl, S. M., Simpson, A. G., Farmer, M. A., Andersen, R. A., Anderson, O. R., Barta, J. R., Bowser, S. S., Brugerolle, G., Fensome, R. A., Fredericq, S. et al. (2005). The new higher level classification of eukaryotes with emphasis on the taxonomy of protists. *J. Eukaryot. Microbiol.* **52**, 399-451.

Altschul, S. F., Madden, T. L., Schaffer, A. A., Zhang, J., Zhang, Z., Miller, W. and Lipman, D. J. (1997). Gapped BLAST and PSI-BLAST: a new generation of protein database search programs. *Nucleic Acids Res.* **25**, 3389-3402.

Arighi, C. N., Hartnell, L. M., Aguilar, R. C., Haft, C. R. and Bonifacino, J. S. (2004). Role of the mammalian retromer in sorting of the cation-independent mannose 6-phosphate receptor. *J. Cell Biol.* **165**, 123-133.

Arnold, K., Bordoli, L., Kopp, J. and Schwede, T. (2006). The SWISS-MODEL workspace: a web-based environment for protein structure homology modelling. *Bioinformatics* **22**, 195-201.

Banerjee, S., Basu, S. and Sarkar, S. (2010). Comparative genomics reveals selective distribution and domain organization of FYVE and PX domain proteins across eukaryotic lineages. *BMC Genomics* **11**, 83.

Berriman, M., Ghedin, E., Hertz-Fowler, C., Blandin, G., Renauld, H., Bartholomeu, D. C., Lennard, N. J., Caler, E., Hamlin, N. E., Haas, B. et al. (2005). The genome of the African trypanosome *Trypanosoma brucei*. *Science* **309**, 416-422.

Bonifacino, J. S. and Glick, B. S. (2004). The mechanisms of vesicle budding and fusion. Cell **116**, 153-166.

Braschi, E., Goyon, V., Zunino, R., Mohanty, A., Xu, L. and McBride, H. M. (2010). Vps35 mediates vesicle transport between the mitochondria and peroxisomes. *Curr. Biol.* **20**, 1310-1315.

Bujny, M. V., Popoff, V., Johannes, L. and Cullen, P. J. (2007). The retromer component sorting nexin-1 is required for efficient retrograde transport of Shiga toxin from early endosome to the trans Golgi network. *J. Cell Sci.* **120**, 2010-2021.

Burkard, G., Fragoso, C. M. and Roditi, I. (2007). Highly efficient stable transformation of bloodstream forms of *Trypanosoma brucei*. *Mol. Biochem. Parasitol.* **153**, 220-223.

Cai, H., Reinisch, K. and Ferro-Novick, S. (2007). Coats, tethers, Rabs, and SNAREs work together to mediate the intracellular destination of a transport vesicle. *Dev. Cell* **12**, 671-682.

Carlton, J. G., Bujny, M. V., Peter, B. J., Oorschot, V. M., Rutherford, A., Arkell, R. S., Klumperman, J., McMahon, H. T. and Cullen, P. J. (2005). Sorting nexin-2 is associated with tubular elements of the early endosome, but is not essential for retromer-mediated endosome-to-TGN transport. *J. Cell Sci.* **118**, 4527-4539.

Chen, D., Xiao, H., Zhang, K., Wang, B., Gao, Z., Jian, Y., Qi, X., Sun, J., Miao, L. and Yang, C. (2010). Retromer is required for apoptotic cell clearance by phagocytic receptor recycling. *Science* **327**, 1261-1264.

Chung, W.-L., Leung, K. F., Natesan, S. K. A., Carrington, M. and Field, M. C. (2008). Ubiquitylation is required for degradation of trans-membrane surface proteins in trypanosomes *Traffic* **9**, 1681-1697.

Collins, B. M. (2008). The structure and function of the retromer protein complex. *Traffic* **9**, 1811-1822.

Collins, B. M., Skinner, C. F., Watson, P. J., Seaman, M. N. and Owen, D. J. (2005). Vps29 has a phosphoesterase fold that acts as a protein interaction scaffold for retromer assembly. *Nat. Struct. Mol. Biol.* **12**, 594-602.

Cullen, P. J. (2008). Endosomal sorting and signalling: an emerging role for sorting nexins. *Nat. Rev. Mol. Cell Biol.* **9**, 574-582.

Dacks, J. B. and Field, M. C. (2004). Eukaryotic cell evolution from a genomic perspective: the endomembrane system. In *Organelles, Genomes and Eukaryote Phylogeny: An Evolutionary Synthesis in the Age of Genomics* (ed. R. P. Hirt and D. S. Horner), pp. 309-334. London: CRC Press.

Dacks, J. B. and Field, M. C. (2007). Evolution of the eukaryotic membrane-trafficking system: origin, tempo and mode. *J. Cell Sci.* **120**, 2977-2985.

Dacks, J. B., Poon, P. P. and Field, M. C. (2008). Phylogeny of endocytic components yields insight into the process of nonendosymbiotic organelle evolution. *Proc. Natl. Acad. Sci. USA* **105**, 588-593.

Dacks, J. B., Peden, A. A. and Field, M. C. (2009). Evolution of specificity in the eukaryotic endomembrane system. *Int. J. Biochem. Cell Biol.* **41**, 330-340.

Damen, E., Krieger, E., Nielsen, J. E., Eygensteyn, J. and van Leeuwen, J. E. (2006). The human Vps29 retromer component is a metallo-phosphoesterase for a cation-independent mannose 6-phosphate receptor substrate peptide. *Biochem. J.* **398**, 399-409.

DeGrasse, J. A., DuBois, K. N., Devos, D., Siegel, T. N., Sali, A., Field, M. C., Rout, M. P. and Chait, B. T. (2009). Evidence for a shared nuclear pore complex architecture that is conserved from the last common eukaryotic ancestor. *Mol. Cell. Proteomics* **8**, 2119-2130.

Devos, D., Dokudovskaya, S., Alber, F., Williams, R., Chait, B. T., Sali, A. and Rout, M. P. (2004). Components of coated vesicles and nuclear pore complexes share a common molecular architecture. *PLoS Biol.* **2**, e380.

Eaton, S. (2008). Retromer retrieves wntless. *Dev. Cell* **14**, 4-6.

Edgar, R. C. (2004). MUSCLE: multiple sequence alignment with high accuracy and high throughput. *Nucleic Acids Res.* **32**, 1792-1797.

Field, M. C. and Carrington, M. (2009). The trypanosome flagellar pocket. *Nat. Rev. Microbiol.* **7**, 775-786.

Field, M. C. and Dacks, J. B. (2009). First and last ancestors: reconstructing evolution of the endomembrane system with ESCRTs, vesicle coat proteins, and nuclear pore complexes. *Curr. Opin. Cell Biol.* **21**, 4-13.

Field, M. C., Gabernet-Castello, C. and Dacks, J. B. (2007a). Reconstructing the evolution of the endocytic system: insights from genomics and molecular cell biology. *Adv. Exp. Med. Biol.* **607**, 84-96.

Field, M. C., Natesan, S. K., Gabernet-Castello, C. and Koumandou, V. L. (2007b). Intracellular trafficking in the trypanosomatids. *Traffic* **8**, 629-639.

George, A., Leahy, H., Zhou, J. and Morin, P. J. (2007). The vacuolar-ATPase inhibitor bafilomycin and mutant VPS35 inhibit canonical Wnt signaling. *Neurobiol. Dis.* **26**, 125-133.

Gokool, S., Tattersall, D. and Seaman, M. N. (2007). EHD1 interacts with retromer to stabilize SNX1 tubules and facilitate endosome-to-Golgi retrieval. *Traffic* **8**, 1873-1886.

Griffin, C. T., Trejo, J. and Magnuson, T. (2005). Genetic evidence for a mammalian retromer complex containing sorting nexins 1 and 2. *Proc. Natl. Acad. Sci. USA* **102**, 15173-15177.

Guindon, S. and Gascuel, O. (2003). A simple, fast, and accurate algorithm to estimate large phylogenies by maximum likelihood. *Syst. Biol.* **52**, 696-704.

Gullapalli, A., Garrett, T. A., Paing, M. M., Griffin, C. T., Yang, Y. and Trejo, J. (2004). A role for sorting nexin 2 in epidermal growth factor receptor down-regulation: evidence for distinct functions of sorting nexin 1 and 2 in protein trafficking. *Mol. Biol. Cell* **15**, 2143-2155.

Gullapalli, A., Wolfe, B. L., Griffin, C. T., Magnuson, T. and Trejo, J. (2006). An essential role for SNX1 in lysosomal sorting of protease-activated receptor-1: evidence for retromer-, Hrs-, and Tsg101-independent functions of sorting nexins. *Mol. Biol. Cell* **17**, 1228-1238.

Haft, C. R., de la Luz Sierra, M., Barr, V. A., Haft, D. H. and Taylor, S. I. (1998). Identification of a family of sorting nexin molecules and characterization of their association with receptors. *Mol. Cell. Biol.* **18**, 7278-7287.

Haft, C. R., de la Luz Sierra, M., Bafford, R., Lesniak, M. A., Barr, V. A. and Taylor, S. I. (2000). Human orthologs of yeast vacuolar protein sorting proteins Vps26, 29, and **35**, assembly into multimeric complexes. *Mol. Biol. Cell* **11**, 4105-4116.

He, X., Li, F., Chang, W. P. and Tang, J. (2005). GGA proteins mediate the recycling pathway of memapsin 2 (BACE). *J. Biol. Chem.* **280**, 11696-11703.

Hettema, E. H., Lewis, M. J., Black, M. W. and Pelham, H. R. (2003). Retromer and the sorting nexins Snx4/41/42 mediate distinct retrieval pathways from yeast endosomes. *EMBO J.* **22**, 548-557.

Hierro, A., Rojas, A. L., Rojas, R., Murthy, N., Effantin, G., Kajava, A. V., Steven, A. C., Bonifacino, J. S. and Hurley, J. H. (2007). Functional architecture of the retromer cargo-recognition complex. *Nature* **449**, 1063-1067.

Hooft, R. W., Vriend, G., Sander, C. and Abola, E. E. (1996). Errors in protein structures. *Nature* **381**, 272.

Hu, Y. H., Warnatz, H. J., Vanhecke, D., Wagner, F., Fiebitz, A., Thamm, S., Kahlem, P., Lehrach, H., Yaspo, M. L. and Janitz, M. (2006). Cell array-based intracellular localization screening reveals novel functional features of human chromosome 21 proteins. *BMC Genomics* **7**, 155.

Hurley, J. H. (2008). ESCRT complexes and the biogenesis of multivesicular bodies. *Curr. Opin. Cell Biol.* **20**, 4-11.

Kama, R., Robinson, M. and Gerst, J. E. (2007). Btn2, a Hook1 ortholog and potential Batten disease-related protein, mediates late endosome-Golgi protein sorting in yeast. *Mol. Cell. Biol.* **27**, 605-621.

Kerr, M. C., Bennetts, J. S., Simpson, F., Thomas, E. C., Flegg, C., Gleeson, P. A., Wicking, C. and Teasdale, R. D. (2005). A novel mammalian retromer component, Vps26B. *Traffic* **6**, 991-1001.

Kim, E., Lee, J. W., Baek, D. C., Lee, S. R., Kim, M. S., Kim, S. H., Imakawa, K. and Chang, K. T. (2008). Identification of novel retromer complexes in the mouse testis. *Biochem. Biophys. Res. Commun.* **375**, 16-21.

Koumandou, V. L., Natesan, S. K., Sergeenko, T. and Field, M. C. (2008). The trypanosome transcriptome is remodelled during differentiation but displays limited responsiveness within life stages. *BMC Genomics* **9**, 298.

Kurten, R. C., Cadena, D. L. and Gill, G. N. (1996). Enhanced degradation of EGF receptors by a sorting nexin, SNX1. *Science* **272**, 1008-1010.

Kurten, R. C., Eddington, A. D., Chowdhury, P., Smith, R. D., Davidson, A. D. and Shank, B. B. (2001). Self-assembly and binding of a sorting nexin to sorting endosomes. *J. Cell Sci.* **114**, 1743-1756.

Laskowski, R. A., MacArthur, M. W., Moss, D. S. and Thornton, J. M. (1993). PROCHECK-A program to check the stereochemical quality of protein structures. *J. Appl. Crystallogr.* **26**, 283-291.

Leung, K. F., Dacks, J. B. and Field, M. C. (2008). Evolution of the multivesicular body ESCRT machinery; retention across the eukaryotic lineage. *Traffic* **9**, 1698-1716.

Lin, S. X., Grant, B., Hirsh, D. and Maxfield, F. R. (2001). Rme-1 regulates the distribution and function of the endocytic recycling compartment in mammalian cells. *Nat. Cell Biol.* **3**, 567-572.

Luthy, R., Bowie, J. U. and Eisenberg, D. (1992). Assessment of protein models with three-dimensional profiles. *Nature* **356**, 83-85.

Mari, M., Bujny, M. V., Zeuschner, D., Geerts, W. J., Griffith, J., Petersen, C. M., Cullen, P. J., Klumperman, J. and Geuze, H. J. (2008). SNX1 defines an early endosomal recycling exit for sortilin and mannose 6-phosphate receptors. *Traffic* **9**, 380-393.

Masuda, M. and Mochizuki, N. (2010). Structural characteristics of BAR domain superfamily to sculpt the membrane. *Semin. Cell Dev. Biol.* **21**, 391-398.

Mizuguchi, K., Deane, C. M., Blundell, T. L., Johnson, M. S. and Overington, J. P. (1998). JOY: protein sequence-structure representation and analysis. *Bioinformatics* **14**, 617-623.

Nakada-Tsukui, K., Saito-Nakano, Y., Ali, V. and Nozaki, T. (2005). A retromerlike complex is a novel Rab7 effector that is involved in the transport of the virulence factor cysteine protease in the enteric protozoan parasite *Entamoeba histolytica*. *Mol. Biol. Cell* **16**, 5294-5303.

Natesan, S. K., Peacock, L., Matthews, K., Gibson, W. and Field, M. C. (2007). Activation of endocytosis as an adaptation to the mammalian host by trypanosomes. *Eukaryot. Cell* **6**, 2029-2037.

Nothwehr, S. F. and Hindes, A. E. (1997). The yeast VPS5/GRD2 gene encodes a sorting nexin-1-like protein required for localizing membrane proteins to the late Golgi. *J. Cell Sci.* **110**, 1063-1072.

Nothwehr, S. F., Bruinsma, P. and Strawn, L. A. (1999). Distinct domains within Vps35p mediate the retrieval of two different cargo proteins from the yeast prevacuolar/endosomal compartment. *Mol. Biol. Cell* **10**, 875-890.

Nothwehr, S. F., Ha, S. A. and Bruinsma, P. (2000). Sorting of yeast membrane proteins into an endosome-to-Golgi pathway involves direct interaction of their cytosolic domains with Vps35p. *J. Cell Biol.* **151**, 297-310.

Pelham, H. R. (1999). SNAREs and the secretory pathway-lessons from yeast. *Exp. Cell Res.* **247**, 1-8.

Popoff, V., Mardones, G. A., Tenza, D., Rojas, R., Lamaze, C., Bonifacino, J. S., Raposo, G. and Johannes, L. (2007). The retromer complex and clathrin define an early endosomal retrograde exit site. *J. Cell Sci.* **120**, 2022-2031.

Pylypenko, O., Lundmark, R., Rasmuson, E., Carlsson, S. R. and Rak, A. (2007). The PX-BAR membrane-remodeling unit of sorting nexin 9. *EMBO J.* **26**, 4788-4800.

Raymond, C. K., Howald-Stevenson, I., Vater, C. A. and Stevens, T. H. (1992). Morphological classification of the yeast vacuolar protein sorting mutants: evidence for a prevacuolar compartment in class E vps mutants. *Mol. Biol. Cell* **3**, 1389-1402.

Reddy, J. V. and Seaman, M. N. (2001). Vps26p, a component of retromer, directs the interactions of Vps35p in endosome-to-Golgi retrieval. *Mol. Biol. Cell* **12**, 3242-3256.

Redmond, S., Vadivelu, J. and Field, M. C. (2003). RNAit: an automated web-based tool for the selection of RNAi targets in *Trypanosoma brucei*. *Mol. Biochem. Parasitol.* **128**, 115-118.

Rojas, R., van Vlijmen, T., Mardones, G. A., Prabhu, Y., Rojas, A. L., Mohammed, S., Heck, A. J., Raposo, G., van der Sluijs, P. and Bonifacino, J. S. (2008). Regulation of retromer recruitment to endosomes by sequential action of Rab5 and Rab7. *J. Cell Biol.* **183**, 513-526.

Ronquist, F. and Huelsenbeck, J. P. (2003). MrBayes 3, Bayesian phylogenetic inference under mixed models. *Bioinformatics* **19**, 1572-1574.

Sali, A. and Blundell, T. L. (1993). Comparative protein modelling by satisfaction of spatial restraints. *J. Mol. Biol.* **234**, 779-815.

Schwarz, D. G., Griffin, C. T., Schneider, E. A., Yee, D. and Magnuson, T. (2002). Genetic analysis of sorting nexins 1 and 2 reveals a redundant and essential function in mice. *Mol. Biol. Cell* **13**, 3588-3600.

Seaman, M. N. (2004). Cargo-selective endosomal sorting for retrieval to the Golgi requires retromer. *J. Cell Biol.* **165**, 111-122.

Seaman, M. N., Marcusson, E. G., Cereghino, J. L. and Emr, S. D. (1997). Endosome to Golgi retrieval of the vacuolar protein sorting receptor, Vps10p, requires the function of the VPS29, VPS30, and VPS35 gene products. *J. Cell Biol.* **137**, 79-92.

Seaman, M. N., McCaffery, J. M. and Emr, S. D. (1998). A membrane coat complex essential for endosome-to-Golgi retrograde transport in yeast. *J. Cell Biol.* **142**, 665-681.

Seaman, M. N., Harbour, M. E., Tattersall, D., Read, E. and Bright, N. (2009). Membrane recruitment of the cargo-selective retromer subcomplex is catalysed by the small GTPase Rab7 and inhibited by the Rab-GAP TBC1D5. *J. Cell Sci.* **122**, 2371-2382.

Shi, J., Blundell, T. L. and Mizuguchi, K. (2001). FUGUE: sequence-structure homology recognition using environment-specific substitution tables and structure-dependent gap penalties. *J. Mol. Biol.* **310**, 243-257.

Small, S. A., Kent, K., Pierce, A., Leung, C., Kang, M. S., Okada, H., Honig, L., Vonsattel, J. P. and Kim, T. W. (2005). Model-guided microarray implicates the retromer complex in Alzheimer's disease. *Ann. Neurol.* **58**, 909-919.

Stamatakis, A. (2006). RAxML-VI-HPC: maximum likelihood-based phylogenetic analyses with thousands of taxa and mixed models. *Bioinformatics* **22**, 2688-2690.

Strochlic, T. I., Setty, T. G., Sitaram, A. and Burd, C. G. (2007). Grd19/Snx3p functions as a cargo-specific adapter for retromer-dependent endocytic recycling. *J. Cell Biol.* **177**, 115-125.

Teasdale, R. D., Loci, D., Houghton, F., Karlsson, L. and Gleeson, P. A. (2001). A large family of endosome-localized proteins related to sorting nexin 1. *Biochem. J.* **358**, 7-16.

Verges, M., Luton, F., Gruber, C., Tiemann, F., Reinders, L. G., Huang, L., Burlingame, A. L., Haft, C. R. and Mostov, K. E. (2004). The mammalian retromer regulates transcytosis of the polymeric immunoglobulin receptor. *Nat. Cell Biol.* **6**, 763-769.

Verges, M., Sebastian, I. and Mostov, K. E. (2007). Phosphoinositide 3-kinase regulates the role of retromer in transcytosis of the polymeric immunoglobulin receptor. *Exp. Cell Res.* **313**, 707-718.

Voos, W. and Stevens, T. H. (1998). Retrieval of resident late-Golgi membrane proteins from the prevacuolar compartment of Saccharomyces cerevisiae is dependent on the function of Grd19p. *J. Cell Biol.* **140**, 577-590.

Wassmer, T., Attar, N., Bujny, M. V., Oakley, J., Traer, C. J. and Cullen, P. J. (2007). A loss-of-function screen reveals SNX5 and SNX6 as potential components of the mammalian retromer. *J. Cell Sci.* **120**, 45-54.

Wassmer, T., Attar, N., Harterink, M., van Weering, J. R., Traer, C. J., Oakley, J., Goud, B., Stephens, D. J., Verkade, P., Korswagen, H. C. et al. (2009). The retromer coat complex coordinates endosomal sorting and dynein-mediated transport, with carrier recognition by the trans-Golgi network. *Dev. Cell* **17**, 110-122.

Whyte, J. R. and Munro, S. (2001). A yeast homolog of the mammalian mannose 6-phosphate receptors contributes to the sorting of vacuolar hydrolases. *Curr. Biol.* **11**, 1074-1078.

Yamazaki, M., Shimada, T., Takahashi, H., Tamura, K., Kondo, M., Nishimura, M. and Hara-Nishimura, I. (2008). Arabidopsis VPS35, a retromer component, is required for vacuolar protein sorting and involved in plant growth and leaf senescence. *Plant Cell Physiol.* **49**, 142-156.